

AD-753 396

THEORETICAL MEINEL BAND RESEARCH

David C. Cartwright, et al

Aerospace Corporation

Prepared for:

Space and Missile Systems Organization

15 November 1972

DISTRIBUTED BY:

NTIS

National Technical Information Service
U. S. DEPARTMENT OF COMMERCE
5285 Port Royal Road, Springfield Va. 22151

AIR FORCE REPORT NO.
SAMSO-TR-72-292

AEROSPACE REPORT NO.
TR-0073(9260-01)-6

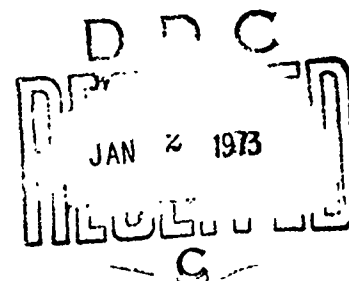
AD753396

THEORETICAL MEINEL BAND RESEARCH

Prepared by D. C. CARTWRIGHT and N. A. FIAMENGO
Space Physics Laboratory

72 NOV 15

Laboratory Operations
THE AEROSPACE CORPORATION



Prepared for SPACE AND MISSILE SYSTEMS ORGANIZATION
AIR FORCE SYSTEMS COMMAND
LOS ANGELES AIR FORCE STATION
Los Angeles, California

APPROVED FOR PUBLIC RELEASE;
DISTRIBUTION UNLIMITED

Revised by
NATIONAL TECHNICAL
INFORMATION SERVICE

51

LABORATORY OPERATIONS

The Laboratory Operations of The Aerospace Corporation is conducting experimental and theoretical investigations necessary for the evaluation and application of scientific advances to new military concepts and systems. Versatility and flexibility have been developed to a high degree by the laboratory personnel in dealing with the many problems encountered in the nation's rapidly developing space and missile systems. Expertise in the latest scientific developments is vital to the accomplishment of tasks related to these problems. The laboratories that contribute to this research are:

Aerodynamics and Propulsion Research Laboratory: Launch and reentry aerodynamics, heat transfer, reentry physics, propulsion, high-temperature chemistry and chemical kinetics, structural mechanics, flight dynamics, atmospheric pollution, and high-power gas lasers.

Electronics Research Laboratory: Generation, transmission, detection, and processing of electromagnetic radiation in the terrestrial and space environments, with emphasis on the millimeter-wave, infrared, and visible portions of the spectrum; design and fabrication of antennas, complex optical systems and photolithographic solid-state devices; test and development of practical superconducting detectors and laser devices and technology, including high-power lasers, atmospheric pollution, and biomedical problems.

Materials Sciences Laboratory: Development of new materials; metal matrix composites and new forms of carbon; test and evaluation of graphite and ceramics in reentry; spacecraft materials and components in radiation and high-vacuum environments; application of fracture mechanics to stress corrosion and fatigue-induced fractures in structural metals; effect of nature of material surfaces on lubrication, photosensitization, and catalytic reactions, and development of prosthesis devices.

Plasma Research Laboratory: Reentry physics and nuclear weapons effects; the interaction of antennas with reentry plasma sheaths; experimentation with thermonuclear plasmas; the generation and propagation of plasma waves in the magnetosphere; chemical reactions of vibrationally excited species in rocket plumes; and high-precision laser ranging.

Space Physics Laboratory: Aeronomy; density and composition of the atmosphere at all altitudes; atmospheric reactions and atmospheric optics; pollution of the environment; the sun, earth's resources; meteorological measurements; radiation belts and cosmic rays; and the effects of nuclear explosions, magnetic storms, and solar radiation on the atmosphere.

THE AEROSPACE CORPORATION
El Segundo, California

ADDITIONAL INFO	
NTIS	Write Section <input checked="" type="checkbox"/>
DDI	215 Unit <input type="checkbox"/>
USPA, 0-270	<input type="checkbox"/>
ADDITIONAL INFO	<input type="checkbox"/>
BY	
A	

UNCLASSIFIED

Security Classification

DOCUMENT CONTROL DATA - R & D

(Security classification of title, body of abstract and indexing annotation must be entered when the overall report is classified)

1 ORIGINATING ACTIVITY (Corporate author) The Aerospace Corporation El Segundo, California		2a REPORT SECURITY CLASSIFICATION Unclassified	
2b GROUP			
3 REPORT TITLE THEORETICAL MEINEL BAND RESEARCH			
4 DESCRIPTIVE NOTES (Type of report and inclusive dates)			
5 AUTHOR(S) (First name, middle initial, last name) David C. Cartwright and Nicholas A. Fiamengo			
6 REPORT DATE 72 NOV 15		7a TOTAL NO OF PAGES 92 87	7b NO OF REFS 84
8a CONTRACT OR GRANT NO F04701-72-C-0073		9a ORIGINATOR'S REPORT NUMBER(S) TR-0073(9260-01)-6	
b PROJECT NO.		9b OTHER REPORT NO(S) (Any other numbers that may be assigned this report) SAMSO-TR-72-292	
c			
d			
10 DISTRIBUTION STATEMENT Approved for public release; distribution unlimited			
11 SUPPLEMENTARY NOTES		12 SPONSORING MILITARY ACTIVITY Space and Missile Systems Organization Air Force Systems Command Los Angeles, California	
13 ABSTRACT The purpose of this theoretical research was to try to develop an accurate theoretical model of the optical excitation, emission, and deactivation properties of the Meinel band system of N_2^+ . A brief review of the interest and objectives of this theoretical research is given and a model for the population of the Meinel bands is proposed. New lifetime data are analyzed by a nonlinear least-squares method to provide the transition moment and its dependence on the internuclear distance. Transition probabilities from $v' = 0-10$ of the $A^2\Pi_u$ state are obtained and found to be significantly different than previously reported. Autoionization and quenching processes involving the A-state are discussed and reasonable estimates for the quenching rates of the A-state by N_2 are given.			

KEY WORDS

Meinel Bands

Meinel Bands, N_2^+

Quenching Rates

Transition Probabilities

Distribution Statement (Continued)

Abstract (Continued)

90
- || -

Air Force Report No.
SAMSC-72-200

Aerospace Report No.
AK-0013(200-01)-6

THEORETICAL MEINEL BAND RESEARCH

Prepared by

D. C. Cartwright and N. A. Fiamengo
Space Physics Laboratory

72 NOV 15

Laboratory Operations
THE AEROSPACE CORPORATION

Prepared for

SPACE AND MISSILE SYSTEMS ORGANIZATION
AIR FORCE SYSTEMS COMMAND
LOS ANGELES AIR FORCE STATION
Los Angeles, California

iii
-111-
Approved for public release; distribution unlimited

FOREWORD

This report is published by The Aerospace Corporation, El Segundo, California, under Air Force Contract No. F04701-72-C-0073. The research was supported and monitored by the Air Force Technical Applications Center (AFTAC/TD-3C), Alexandria, Virginia 22313, under Project Authorization No. T/2302/Z/SAMSO.

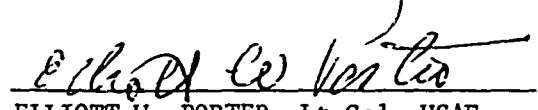
The authors wish to thank Jim Peterson and John Moseley of Stanford Research Institute, and Redus Holland and Bill Maier of Los Alamos Scientific Laboratory for providing the experimental results that served as the foundation for the work reported herein. Special thanks also go to these individuals for stimulating and interesting discussions on the interpretation of these data. Special thanks also go to Major Gary Culp (USAF) who suggested this problem and who expertly and enthusiastically coordinated the fruitful interchange of ideas between the experimental and analytical efforts.

This report, which documents research carried out from 1 October 1971 through 30 June 1972, was submitted for review and approval on 20 October 1972 to Lt Col Elliott W. Porter, DYX.

Approved


G. A. Paulikas, Director
Space Physics Laboratory

Publication of this report does not constitute Air Force approval of the report's findings or conclusions. It is published only for the exchange and stimulation of ideas.


ELLIOTT W. PORTER, Lt Col, USAF
Asst Dir, Development Directorate
Deputy for Technology

CONTENTS

FOREWORD	ii
ABSTRACT	iii
I.	INTRODUCTION	1
II.	MODEL FOR POPULATION OF MEINEL BANDS	7
III.	MEINEL BAND TRANSITION PROBABILITIES	13
	A. Introduction	13
	B. Theory	15
	C. Numerical Techniques	20
	D. Results for the Meinel System of N_2^+	24
IV.	AUTOIONIZATION	41
V.	QUENCHING OF THE B $^2\Sigma_u^+$ AND A $^2\Pi_u$ STATES	49
	A. Lifetimes for the B $^2\Sigma_u^+$ State	49
	B. Quenching Rates for the B-State	53
	C. Quenching Rates for the A-State	57
VI.	EXTRACTION OF LIFETIMES FROM FLUORESCENT DECAY DATA	63
	A. Introduction	63
	B. Method	63
	C. Usage and Interpretation	66
	D. Examples	70
VII.	CONCLUSIONS	83

FIGURES

1.	Photon absorption spectrum of N_2 between 650 and 800 Å, showing the autoionizing Rydberg states	9
2.	Measured inverse lifetimes as a function of v' for the $A^2\Pi_u$ state of N_2^+	25
3.	Ratio of inverse lifetime to $\sum_{v'} \nu_{v',v'}^3 q_{v',v'}$ as a function of v' for the A-state of N_2^+	27
4.	Transition moment for the Meinel band system of N_2^+ as a function of the internuclear distance as determined from the new lifetime data	30
5.	Comparison of the "electronic" portion of the band strength determined in this research with previous results	32
6.	Potential energy curves for the N_2^+ states as calculated using the GVB method (solid lines) and the Hartree-Fock method (dashed lines)	44
7.	Fluorescent decay data and the best fit to them for the NI doublet at 1200 Å	71
8.	Fluorescent decay data and the best fit to them for the (3, 1) + (9, 6) bands of the N_2 1 st positive band system	73
9.	Low-pressure fluorescent decay data and the best fit to it for the (2, 0) N_2^+ Meinel band	74
10.	Same as Fig. 9, but at higher pressure and for which two components are present	75
11.	Same as Fig. 10, but at lower pressure and higher beam current	77

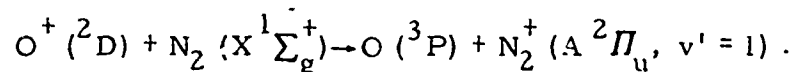
Preceding page blank

TABLES

I.	Optimum Two-Parameter Coefficients in Eq. (13) for Case I and II Data	28
II.	Oscillator Strengths, Transition Probabilities, and Band . . Origin Wavelengths for the Meinel System of N_2^+	35
III.	Lifetimes for $B^2\Sigma_u^+$ of N_2^+	50
IV.	Transition Probabilities for the First Negative System of N_2^+	52
V.	Quenching Rates for $B^2\Sigma_u^+$ (10^{-10} cm ³ /sec)	54
VI.	Quenching Rates for the Meinel Bands Obtained from Data of Simpson and McConkey and Transition Probabilities of Sec. II.	58
VII.	Quenching of CO^+ ($A^2\Pi$) by CO	60
VIII.	Fluorescent Decay of the 1200 A Doublet of NI	70

I. INTRODUCTION

The Meinel band system of N_2^+ , $A^2\Pi_u - X^2\Sigma_g^+$, is not only one of the strongest emission features in normal auroras, but also might well play a role in chemical reactions and charge transfer processes which occur in the upper atmosphere. Observations¹ indicate that in normal auroras, the First Positive system is the strongest emission feature, the Meinel system about a factor of two weaker, and the O_2 Infrared Atmospheric about 60 percent of the Meinel system. Anomalies in the rotational and vibrational distributions of the auroral Meinel bands have led to the suggestion² that $v' = 1$ of the $A^2\Pi_u$ state is populated by the charge transfer process



Recent laboratory measurements on the quenching of the $B^2\Sigma_u^+$ state of N_2^+ suggest³ that one of the products of the quenching might be the A-state of N_2^+ . The Meinel band system has also been detected⁴ in the dayglow where it appears to be populated by both photoionization and the O^+ charge transfer process.

The Meinel band system was discovered by Meinel⁵ in the study of auroral emissions and following a series of refined experiments⁶, the correct vibrational numbering and location of the $A^2\Pi_u$ state was obtained. Fedorova⁷ and coworkers have made a series of auroral and laboratory measurements on the Meinel band system in an effort to determine its radiative and excitation properties, but have had considerable difficulty obtaining consistent results

because of strong quenching effects. It is worth noting that the spectral region 0.95 to 2.0 μm in both the aurora and dayglow has been little studied due to the relatively poor response of detectors in this spectral region and yet it contains some of the most intense spectral features. However, Vallance-Jones and Gattinger,⁸ and Harrison⁹ have recently begun a systematic study of the auroral spectrum out to about 2.5 μm .

Before measurements of the atmospheric emission features can be utilized to characterize the properties of the source of the excitations, the fundamental excitation and radiative properties of the band system of interest must be known. In the case of the First Positive system of N_2 , the excitation and radiative processes are well enough known from laboratory measurements to allow calculations to be made on auroral processes.¹⁰ In the case of the Meinel band system, the laboratory experiments have not yet obtained reliable excitation cross sections and only very recently, through the use of time-of-flight techniques, have the natural lifetimes for the $\text{A } ^2\Pi_u$ state been determined.^{11,12} The fundamental information needed are (i) the transition probabilities, (ii) the excitation cross sections, and (iii) the quenching rates, for the lowest 6 or 7 vibrational levels of the $\text{A } ^2\Pi_u$ state. With this basic information it is possible to evaluate the importance of secondary excitation processes for the A-state such as quenching from the B-state and charge transfer with O^+ , which are expected to be important at lower altitudes.

There have recently been a variety of experiments conducted on N_2^+ with the aim of obtaining one or more of the three fundamental properties for the Meinel system mentioned above. The details of these experiments will

not be discussed in detail here since the experimental groups¹¹⁻¹³ now working on the properties of the Meinel system will address these questions more completely. However, it is worth mentioning the peculiarities which have been observed for the Meinel system during the experimental work. The difficulty which has plagued all the laboratory experiments on the Meinel system, except the time-of-flight lifetime studies, is a combination of the large quenching cross section for the A-state and its relatively long lifetime. Conventional fluorescent decay experiments could not be conducted at low enough pressure to permit reliable extrapolation to zero pressure. In addition, pressure dependence of the measured intensity in these experiments generally cannot be described by a Stern-Volmer type relation and in some previous cases, certain properties of the apparatus employed seemed to affect the measured quantities.

The objective of this theoretical research was to go as far as possible toward developing a consistent theoretical model of the optical excitation, emission and deactivation properties of the N_2^+ Meinel molecular band system excited by electrons. The goal was to develop a better understanding and prediction of:

- a) Excitation Paths
- b) Excitation Cross Sections
- c) Emission Paths and Processes
- d) Emission Cross Sections
- e) Collisional Quenching Cross Sections
- f) Radiative Lifetimes
- g) Absolute Fluorescence Efficiencies

for the (0, 0), (1, 0), (2, 0) and (3, 1) N_2^+ Meinel bands. A good deal of understanding and information about the processes listed above covering the N_2^+ Meinel band system has resulted from this theoretical study and the related experimental research. The model which will be discussed below (Section II) appears to explain the excitation paths of the Meinel system and hence satisfy goal (a) above. The radiative properties and natural lifetimes of the lowest ten vibrational levels are now well understood (see Section III) which fulfills goal (f). The information available on the quenching of the N_2^+ states (Section V) suggests a model which, although not yet completed, indicates that goal (e) on the quenching cross sections may be fulfilled in the near future. The experimental work being done at Utah State should help considerably on this important problem. The experimental work done by the Los Alamos group and that which is about to be done at Utah State University¹³ on the excitation cross sections should fulfill goals (b) through (d). When these theoretical and experimental findings are combined, it should be possible to obtain the fluorescence efficiencies for the four Meinel bands desired.

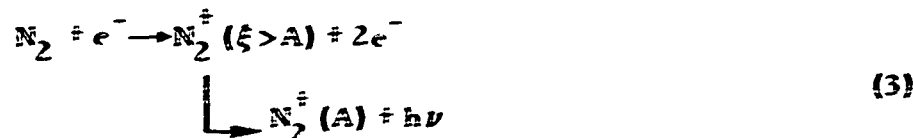
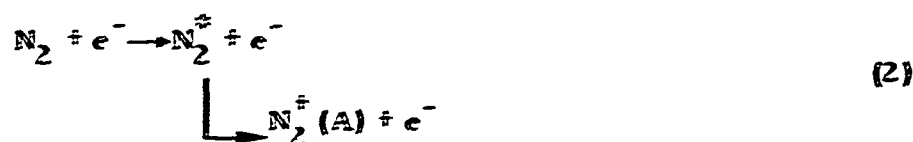
REFERENCES FOR SECTION I

1. A. Vallance Jones, *Space Science Reviews* 11, 776 (1971).
2. A. Onholt, *J. Atmos. Terr. Phys.* 10, 520 (1957).
3. F. J. Comes and F. Speier, *Z. Naturforsch* 26A, 1998 (1971).
4. L. Wallace and A. L. Broadfoot, *Planet. Space Sci.* 17, 975 (1969).
5. A. B. Meinel, *App. J.* 112, 562 (1950); *ibid* 114, 431 (1951).
6. A review of the auroral and airglow work done prior to 1961 is contained in J. W. Chamberlain, *Physics of the Aurora and Airglow*, Academic Press, New York (1961). The more recent measurements are summarized in references 1, 7 and 8.
7. N. I. Fedorova, *Geomag. and Aeronomy* 1, 622 (1961); *Aurora and Airglow*, edited by V. I. Krasovsky, IGY Program, Section IV, No. 10, NASA TT-F-204 (1964), p. 140; *Geomag and Aeronomy* 11, 535 (1971).
8. A. Vallance Jones and R. L. Gattinger, *The Radiating Atmosphere* (ed. by B. M. McCormac) D Reidel Publ. Co., Dordrecht-Holland (1971).
9. A. W. Harrison, *Can. J. Phys.* 47, 599 (1969); *ibid* 50, 500 (1972).
10. D. C. Cartwright, S. Trajmar and W. Williams, *J. Geophys. Res.* 76, 8368 (1971).
11. R. F. Holland and W. B. Maier, II, *J. Chem. Phys.* 56, 229 (1972); W. B. Maier, II and R. F. Holland, *Bull. Am. Phys. Soc.* 17, 695 (GE8) (1972).

12. J. R. Peterson and J. Moseley, to be published (1972).
13. W. R. Pendleton, Jr., and L. D. Weaver, Utah State University,
AFTAC Project Authorization Number VT/1303.

II. MODEL FOR POPULATION OF MEINEL BANDS

The excitation of the Meinel bands by electron bombardment of N_2 could proceed by three possible processes:



Process (1) represents direct excitation of one of the bound electrons of N_2 into the ionization continuum of the A-state and is usually called "direct" excitation of the A-state. Process (2) represents excitation of N_2 to a Rydberg state which is imbedded in the ionization continuum and can then autoionize into the A-state. Process (3) represents excitation (direct or autoionization) into a state of N_2^+ which can energetically cascade into the A-state. The charge transfer process with $O^+(^2D)$ producing $N_2^+(A)$ is not considered here.

Process (1) has in the past been considered as the only important production mechanism of $N_2^+(A)$. This belief was based largely on the fact that $N_2^+(B)$, at least for the lowest two vibrational levels, was found to follow the direct excitation process. However, for the $N_2^+(A)$, the situation seems more complicated. O'Neil and Davidson¹ concluded from their measurements that the lower vibrational levels of the A-state were populated by a dual excitation

process. Holland and Maer, ² using a different experimental technique, have found that the experimental excitation cross sections for $v' = 4$ through $v' = 7$, relative to that for (2, 0), are larger than that predicted by direct excitation. This evidence indicates that there is an excitation process in addition to the direct process which is operative for producing the A-state.

Theoretical considerations and recent experimental results from photoelectron spectroscopy (Section IV) suggest that a combination of processes (2) and (3) play a role in population of the A-state. Autoionization is clearly operative in forming N_2^+ states as has been shown by the work of Cook and Metzger ³ who found that essentially all of the major absorption peaks also autoionized. Some feeling for the magnitude of the autoionization process can be obtained by comparing the peaks with the continuum in Fig. 1, which shows the absorption spectrum ⁴ of N_2 as a function of wavelength. The peaks represent different members of Rydberg series converging to vibrational levels of the various ion states. The members of the various series are indicated along the top of the figure. Since each of these peaks autoionizes, ³ it is clear that they contribute an appreciable amount to the total production of ion states.

Cascade from higher electronic states, or from any vibrational levels that are energetically above a given level of the A-state [e.g., $X(v' \geq 5)$] are also a possible population mechanism for the A-state. The Janin-d'Incan ($D^2 \Pi_g - A^2 \Pi_u$) system is well known as is the Second Negative ($C^2 \Sigma_u^+ - X^2 \Sigma_g^+$) system. ⁵ The Janin-d'Incan transitions tend to populate many vibrational levels of the A-state although the tabulated transitions mainly terminate on

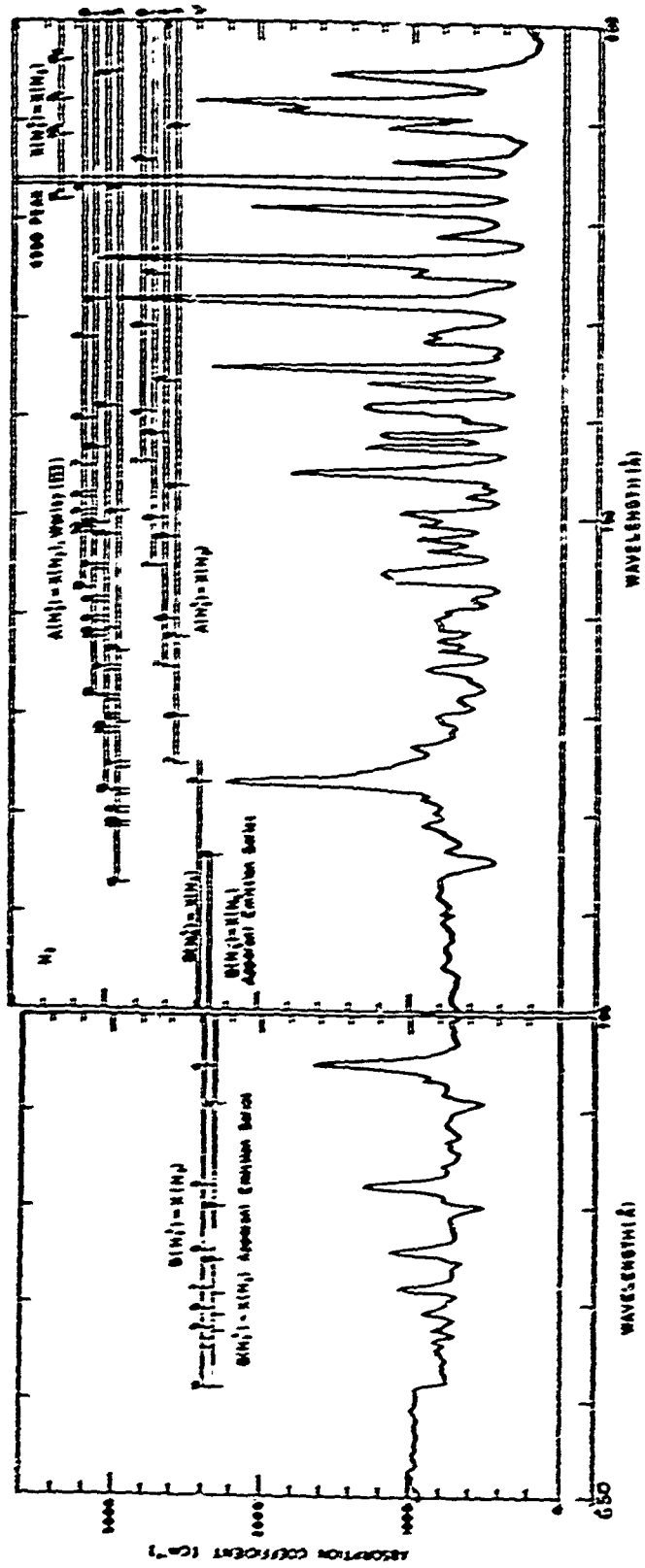


Fig. 1. Photon absorption spectrum of N₂ between 650 and 800 Å, showing the autoionizing Rydberg states.

A-levels less than about 8. The strongest transitions for the Second Negative system terminate⁵ on levels of the X-state greater than $v'' = 5$.

The model that suggests itself for the production of the vibrational population in the A-state involves (i) population of vibrational levels of the X-state greater than four by autoionization and cascade from the C-state, ii) population of higher levels of the A-state by cascade from the D-state, and perhaps some autoionization, and iii) intrasystem cascading between vibrational levels of the X and A states to produce the final vibrational population of the A-state. The non Stern-Volmer quenching which has been observed¹ for certain Meinel transitions could be a result of the quenching of those population processes other than direct excitation. To determine the applicability of this model requires that additional theoretical and experimental work be conducted on the Meinel system. The theoretical work required to understand the processes taking place in the Meinel system was considered to consist of three phases. Phase I was the determination of the transition probabilities and oscillator strengths for the Meinel system. These were felt to be the most important quantities in understanding the Meinel system and they were obtained during this research period. Phase II was formulated to consist of the understanding of the various excitation processes for the levels of the A-state. A good deal of progress has been made in dealing with the autoionization process and this is discussed in Section IV. Phase III is the understanding of the quenching processes in the A-state and thus the fluorescence efficiency of the Meinel band system.

REFERENCES FOR SECTION II

1. R. O'Neil and G. Davidson, AFCRL-67-0277, ASE-1602, American Science and Engineering, Inc., Cambridge, Mass., (1968).
2. R. F. Holland and W. B. Maier, II, J. Chem. Phys. 56, 5229 (1972).
3. G. R. Cook and P. H. Metzger, J. Chem. Phys. 41, 321 (1964).
4. R. E. Huffman, Y. Takaka and J. C. Larrabee, J. Chem. Phys. 39, 910 (1963).
5. L. Wallace, App. J. Supp. 6, 445 (1962).

III. MEINEL BAND TRANSITION PROBABILITIES

A. INTRODUCTION

The Meinel band system of N_2^+ , $A^2\Pi_u - X^2\Sigma_g^+$, was first identified in auroral spectra¹ and has since been the subject of numerous studies² of auroral emission features because of its strength and possible population by $O^+(^2D)$ charge exchange^{2a, 3} with $N_2(X^1\Sigma_g^+)$. Accurate measurements of the lifetimes for vibrational levels $v' = 2-5$ have recently been reported by Holland and Maier⁴, for $v' = 9$ by Maier and Holland,⁵ and for levels $v' = 1-8$ by Peterson and Moseley⁶ (preceding paper). There is excellent agreement between the two sets of measurements for those levels which were measured in both experiments. The papers by Holland and Maier,⁴ and by Peterson and Moseley⁶ contain a discussion of the earlier lifetime measurements and the comparison with their new results. The recent theoretical paper on electronic transition probabilities by Popkie and Henneker⁷ contains an excellent bibliography of the other experimental work which has been done on the Meinel band system. However, many of the basic properties relating to the Meinel system such as the population mechanisms and quenching cross sections are still unknown, which makes the interpretation of atmospheric processes involving this N_2^+ system somewhat uncertain.

Most of the previous attempts to extract the internuclear dependence of the band strength⁸ of the Meinel system from auroral intensities⁹ or laboratory relative intensities¹⁰ have been unsuccessful because of the long lifetimes for the levels of the A-state and the presence of overlapping bands from the N_2 First-Positive band system. Holland and Maier⁴ obtained some

Preceding page blank

information about the internuclear dependence over a small wavelength interval from their ion-beam measurements. Popkie and Henneker⁷ combined the lifetime measurements of O'Neil and Davidson,¹¹ and of Hollstein et al,¹² with the intensity measurements of Stanton and St. John¹³ to estimate the band strength dependence on internuclear distance. However, the lifetimes of the levels of the A-state were not well enough known at the time they did their work for them to establish the correct absolute value or the dependence over an extended range in the internuclear distance. Popkie and Henneker also reported ab initio calculations of the transition moments^{8b} obtained by employing Hartree-Fock wavefunctions.

In this paper, the new lifetime measurements of Holland and Maier,⁴ Maier and Holland,⁵ and Peterson and Moseley,⁶ have been used to extract the transition moment and its dependence on internuclear distance. The data were analyzed by expanding the electronic portion of the molecular dipole strength as a polynomial in the internuclear distance, rather than applying the r-centroid method to the square of the transition moment. The resulting band strengths are considerably different from those derived previously by others. In addition to providing accurate transition probabilities and oscillator strengths for the Meinel band system, these results can be used to obtain reliable values for transition probabilities from levels $v' = 0$ and 9, and hence their lifetimes, for which no experimental data exist.

B. THEORY

A thorough discussion of the theory of molecular electronic-vibrational transition probabilities is given by Henneker and Popkie¹⁴ in paper I of their series dealing with the calculation of transition probabilities in diatomic molecules, and the relationship of these molecular properties to absolute rotational line intensities is discussed by Tatum^{8a} and by Schadee.^{15,16} The Einstein coefficient describing a spontaneous transition from an upper (Γ') to a lower (Γ'') single rotational state can be written (atomic units) as^{14,16}

$$A_{\Gamma' \Gamma''} = \frac{4^3}{3c^3 a_0^3 m_e^3} \Delta E_{\Gamma' \Gamma''}^3 \frac{S_{\Gamma' \Gamma''}}{(2J' + 1)} \quad (1)$$

In Eq. (1), the energy separation, $\Delta E_{\Gamma' \Gamma''}$, and the line strength, $S_{\Gamma' \Gamma''}$, are in atomic units.¹⁷ By convention, the upper state quantities are denoted by single prime and those for the lower by double primes. The quantity a_0 is the Bohr radius, and the others have their usual meaning.^{17b} Denoting the electronic, vibrational and rotational quantum numbers by n , v and J , respectively, and the spin and parity substates^{8b,16} by Σ and p , then the quantity $S_{\Gamma' \Gamma''}$ appearing in Eq. (1) is the dipole-length form for the line strength of the transition between single rotational states,¹⁶ $\Gamma' = n'v'\Sigma'p'J'$ and $\Gamma'' = n''v''\Sigma''p''J''$. It is usually a good approximation to neglect the interaction of the rotational motion with the electronic-vibrational motions, in which case the total line strength can be factored into

$$S_{\Gamma\Gamma''} = S_{\Sigma}^{\Sigma''} \frac{\sum_{p'p''} \sum_{p'J'} \left| \mathcal{Q}_{n'v'\Sigma'p'}^{n''v''\Sigma''p''} \right|^2}{(2 - \delta_{0,\bar{\Lambda}})(2S' + 1)} = S_{\Sigma' p' J'}^{\Sigma'' p'' J''} \frac{S_{n'v'}^{n''v''}}{(2 - \delta_{0,\bar{\Lambda}})(2S' + 1)} \quad (2)$$

The first factor on the right-hand side of Eq. (2) is the Hönl-London factor, normalized so that¹⁶

$$\sum_{J''} \sum_{\Sigma''} \sum_{p'p''} S_{\Sigma' p' J'}^{\Sigma'' p'' J''} = (2 - \delta_{0,\bar{\Lambda}}) (2S' + 1) (2J' + 1) \quad (3)$$

The symbol $\bar{\Lambda}$ is the least of the quantities Λ' and Λ'' involved in the transition, and has been defined this way to insure that the line strength has the desired properties. If the transition involves a Σ -state, $(2 - \delta_{0,\bar{\Lambda}}) = 1$, but it equals 2 for all other transitions. The second factor in Eq. (2) is the square of the electronic-vibrational transition moment, summed and averaged over the final and initial degenerate levels, respectively. Within the framework of Schadee's electronic-vibration degeneracy concept,¹⁶ the degeneracies are taken to be the parity and spin substates. The quantity $S_{n'v'}^{n''v''}$ is customarily called the band strength.^{8a} It is noted that because of this factorization and the normalization of the Hönl-London factors, the transition probability connecting two electronic-vibrational states reduces to (atomic units)

$$A_{n'v'}^{n''v''} = \frac{4e^4}{3c^3 a_0^3 m_e^2} \Delta E_{v'v''}^3 \frac{S_{n'v'}^{n''v''}}{(2 - \delta_{0,\Lambda'}) (2S' + 1)} \quad (4)$$

and in cgs units, is

$$A_{n'v'}^{n''v''} = \frac{64 \pi^4}{3h} \nu_{v'v''}^3 \frac{S_{n'v'}^{n''v''}}{(2 - \delta_{0,\Lambda'}) (2S' + 1)} \quad (5)$$

where $\nu_{v'v''}$ is the energy separation between ($n'v'$) and ($n''v''$) in wavenumbers (cm^{-1}). These transition probabilities are independent of the initial rotational state because of the assumption stated earlier of no coupling between the rotational and the electronic-vibrational motions.

The band strength, defined here by Eq. (2) to include the summation over the parity and spin substates, is the fundamental quantity that characterizes the electronic-vibrational transition. It can be written in many equivalent forms¹⁴ by using the commutation relations between the position coordinates and their conjugate momenta. The approach employed here, however, utilizes just the dipole-length formulation because that is the form most frequently employed¹⁸ in the interpretation of experimental data.

The natural lifetime, $\tau_{v'}$, of any particular vibrational level, v' , of the excited electronic state is related to the decay constant, $A_{n'v'}^{n''}$, by

$$\frac{1}{\tau_{v'}} = A_{n'v'}^{n''} \equiv \sum_{v''} A_{n'v'}^{n''v''} \quad (6)$$

and the absorption band oscillator strength is given by¹⁶

$$f_{n'v'}^{n''v''} = \frac{2}{3} \Delta E_{v'v''} S_{n'v'}^{n''v''} \quad (\text{atomic units}) \quad (7)$$

$$= \frac{8\pi^2 m e}{3 h e^2} \nu_{v'v''} \frac{S_{n'v'}^{n''v''}}{(2 - \delta_{0\Lambda''})(2S'' + 1)} \quad (\text{cgse units}) \quad (8)$$

The analysis of experimental data to obtain information about the electronic-vibrational interaction has been the subject of a good deal of research the past few years, with the majority of the discussion centered around the use of the *r*-centroid approximation.^{18,19} This approximation was introduced to quantitatively account for the fact that the electronic portion of the transition moment^{8b} varies with internuclear distance for many transitions in diatomic molecules. This method of dealing with electronic-vibrational coupling is generally successful¹⁹ from an empirical standpoint, but has been criticized²⁰ because of its weak theoretical foundation and the difficulty of interpreting the *r*-centroid as an average internuclear distance. Employing the matrix notation and suppressing the summation over the degenerate substates, the band strength can be written in terms of the transition moment as (cgse units)

$$S_{n'v'}^{n''v''} = \left| \langle v' | M(R) | v'' \rangle \right|^2 \quad (9)$$

$$= \left| \langle v'n' | -\sum_l e \frac{\vec{r}_l}{l} | v''n'' \rangle \right|^2, \quad (10)$$

where \vec{r}_l denotes the coordinates of the electrons in a molecular-fixed frame, e is the electron charge, and the integration is taken over all electron coordinates, but only the radial coordinates of the nuclei. The customary r -centroid approximation writes Eq. (9) as

$$S_{n'v'}^{n''v''} = (\alpha + \beta r_{v'v''} + \gamma r_{v'v''}^2 + \dots)^2 q_{v'v''} \\ = R_e^2 (r_{v'v''}) q_{v'v''} \quad (11)$$

where $q_{v'v''}$ is the Franck-Condon factor¹⁸ and $r_{v'v''}$ is the r -centroid, defined in terms of the internuclear distance by

$$r_{v'v''} = \frac{\langle v' | R | v'' \rangle}{\langle v' | v'' \rangle} \quad (12)$$

Rather than employing the r -centroid approximation, one may simply expand the electronic portion of the transition moment in Eq. (9) as a power series in the internuclear distance

$$M(R) = \sum_{i=0} a_i R^i \quad (13)$$

in which case Eq. (9) becomes

$$S_{n'v'}^{n''v''} = \left[a_0 \langle v' | v'' \rangle + a_1 \langle v' | R | v'' \rangle + a_2 \langle v' | R^2 | v'' \rangle + \dots \right]^2 \quad (14)$$

As emphasized by Klemsdal,^{20e} this latter approach not only is free of the assumptions incorporated into the r-centroid approximation, which have been shown²⁰ to fail in some cases, but also permits a direct comparison of the obtained transition moment with that predicted by theory.

This approach of utilizing an expansion in terms of matrix elements rather than the r-centroid has been employed by Jain and Sahni^{20b, d} and by Popkie and Henneker⁷ in their analyses of intensity data to obtain the inter-nuclear dependence of the transition moment, and has also been used in the present analysis of the lifetime data.

C. NUMERICAL TECHNIQUES

The extraction of the internuclear distance dependence of the transition moment from lifetime data requires the solution of a nonlinear problem when using either the r-centroid approximation or the matrix approach. This is because the lifetime is related to a sum of transition probabilities, Eq. (6), which are proportional to the square of the transition moment, and hence not linearly related to the unknown coefficients. This is in contrast to intensity data, which are proportional to a single transition probability, and which allows the construction of a linear relationship between the data and the transition moment itself by taking the square root of both sides of the appropriate equation. The method employed in this study to determine the transition moment was the following. Combining Eqs. (14), (4) and (6), the relationship between the lifetime and the transition moment becomes

$$\frac{1}{\tau_{v^n}} = \frac{64\pi^4}{3h} \frac{1}{(2 - \delta_{0A})(2S^n + 1)} \sum_{v^m} \rho_{v^n v^m}^3 x$$

$$\left[a_0 \langle v^n | v^m \rangle + a_1 \langle v^n | E | v^m \rangle + a_2 \langle v^n | E^2 | v^m \rangle + \dots \right]^2 \quad (15)$$

The unknown parameters, a_i , were determined by minimizing the weighted sum of the squares of the residuals, χ^2 , defined by²¹

$$\chi^2 = \sum_{j=1}^N \left[\frac{1}{\sigma_j^2} \left[\frac{1}{\tau_j} - A_j^c \right] \right]^2 \quad (16)$$

where the σ_j are the uncertainties (standard deviations) in the data ($1/\tau_j$), N is the number of data points, and the A_j^c are the calculated decay constants. It is noted that because of the inverse relationship between the lifetime and the decay constant, equal uncertainties in all the measured lifetimes become unequal uncertainties in the decay constants and therefore vary from one vibrational level to another.

The solution of the nonlinear equation (15) to obtain the parameters (a_i) from the measured lifetimes was accomplished by using the differential corrector, or linearization procedure.²² The essence of this method is the Taylor's series expansion of the function which contains the parameters, in the unknown parameters, and the retention of terms through the first derivatives. This approach results in one equation for each unknown parameter, which is still nonlinear in that parameter, but is now linear in the change in that parameter. If there are B parameters to be determined, then the resulting

equations for the change in the parameters can be rearranged²³ into the matrix form

$$\underline{C} \underline{\delta a} = \underline{b} \quad (17)$$

or

$$\begin{bmatrix} \sum_{v'} \frac{1}{\sigma_{v'}^2} \left(\frac{\partial A_{v'}}{\partial a_0} \right)^2 & + \dots & + \sum_{v'} \frac{1}{\sigma_{v'}^2} \frac{\partial A_{v'}}{\partial a_0} \frac{\partial A_{v'}}{\partial a_B} \\ \sum_{v'} \frac{1}{\sigma_{v'}^2} \frac{\partial A_{v'}}{\partial a_0} \frac{\partial A_{v'}}{\partial a_1} & + \dots & + \sum_{v'} \frac{1}{\sigma_{v'}^2} \frac{\partial A_{v'}}{\partial a_1} \frac{\partial A_{v'}}{\partial a_B} \\ \vdots & & \vdots \\ \sum_{v'} \frac{1}{\sigma_{v'}^2} \frac{\partial A_{v'}}{\partial a_0} \frac{\partial A_{v'}}{\partial a_B} & + \dots & + \sum_{v'} \frac{1}{\sigma_{v'}^2} \left(\frac{\partial A_{v'}}{\partial a_B} \right)^2 \end{bmatrix} \begin{bmatrix} \delta a_0 \\ \delta a_1 \\ \vdots \\ \delta a_B \end{bmatrix} = \begin{bmatrix} \sum_{v'} \frac{1}{\sigma_{v'}^2} \frac{\partial A_{v'}}{\partial a_0} D_{v'} \\ \sum_{v'} \frac{1}{\sigma_{v'}^2} \frac{\partial A_{v'}}{\partial a_1} D_{v'} \\ \vdots \\ \sum_{v'} \frac{1}{\sigma_{v'}^2} \frac{\partial A_{v'}}{\partial a_B} D_{v'} \end{bmatrix}$$

where \underline{C} is a symmetric matrix, $A_{v'}$ is the decay constant for level v' , calculated with the assumed values for the parameters, δa_i is the change in the i^{th} parameter, and $D_{v'} = \frac{1}{\sigma_{v'}} \left[A_{v'} - \frac{1}{\tau_{v'}} \right]$ is the weighted residual calculated for level v' with the assumed parameters. The solutions of the matrix equation (17) are the changes in the parameters (δa_i), and from these, a new improved estimate for the parameters can be calculated using

$$a_i = a_i + \delta a_i \quad (i = 1, \dots, B) \quad (18)$$

These improved estimates for the parameters can again be inserted into Eq. (17) and the procedure of solving for the change in the parameters repeated

until the magnitude of the changes in the parameters has decreased to an acceptably low level. Some care must be exercised in the choosing of the initial guesses for the unknown parameters to insure convergence to the true, rather than a local, minimum in χ^2 . It was found that reasonable initial guesses for the nonlinear parameters were obtained by first solving the linear problem formed by expanding the band strength itself (i. e., the square of the transition moment) according to the r-centroid approximation

$$S_{n'v'}^{n''v''} = q_{v'v''} (\alpha_0 + \alpha_1 r_{v'v''}) , \quad (19)$$

where $q_{v'v''}$ is the Franck-Condon factor, $r_{v'v''}$ is the r-centroid, and α_0 and α_1 were determined. In this case the unknown parameters (α_i) are linearly related to the data points and can be obtained by a straightforward application of the leastsquares method. Initial estimates for the unknown parameters (a_i) in the nonlinear problem were obtained from the values of α_0 and α_1 in Eq. (19) according to

$$a_0 = \sqrt{\alpha_0} , \quad a_1 = \frac{\alpha_1}{2 a_0} , \quad a_2 = 0 . \quad (20)$$

The Franck-Condon factors and r-centroids were calculated numerically²⁴ from RKR potential energy curves obtained from spectroscopic data on N_2^+ provided by Albritton et al.²⁵ The matrix elements were obtained by making the appropriate modifications in Zare's²⁴ original programs.

By the use of matrix methods, which return the inverse of the curvature matrix \underline{C} ,

$$\underline{\epsilon} = \underline{C}^{-1}, \quad (21)$$

where \underline{C} is defined by Eq. (17), the uncertainties in each of the parameters a_i due to the uncertainties in the basic data and the quality of the fit can be obtained from²⁶

$$\sigma_{a_i} = \epsilon_{ii} \quad (22)$$

D. RESULTS FOR THE MEINEL SYSTEM OF N_2^+

1. The Transition Moment

The method described in the previous section has been applied to the analysis of the new lifetime measurements of Holland and Maier,⁴ of Peterson and Moseley,⁶ and of Maier and Holland⁵ which include levels $v' = 1-8$ and $v' = 10$. Although the lifetime is the measured quantity, it is the inverse of the lifetime that is directly related to the band strength. Figure 2 summarizes the experimental measurements²⁷ on the lifetimes for the vibrational levels of the Meinel band system, in which the decay constant (inverse lifetime) is plotted as a function of the vibrational quantum number. Also shown in the figure (right-hand ordinate) is the quantity $\sum_{v''} \nu_{v'v''}^3 q_{v'v''}$ because some indication as to the variation of the transition moment with internuclear distance can be obtained by comparing this quantity with $1/\tau_{v'}$. That is, if there were no variation of the transition moment with internuclear distance, these two curves would be parallel. This qualitative comparison can be made more quantitative by plotting

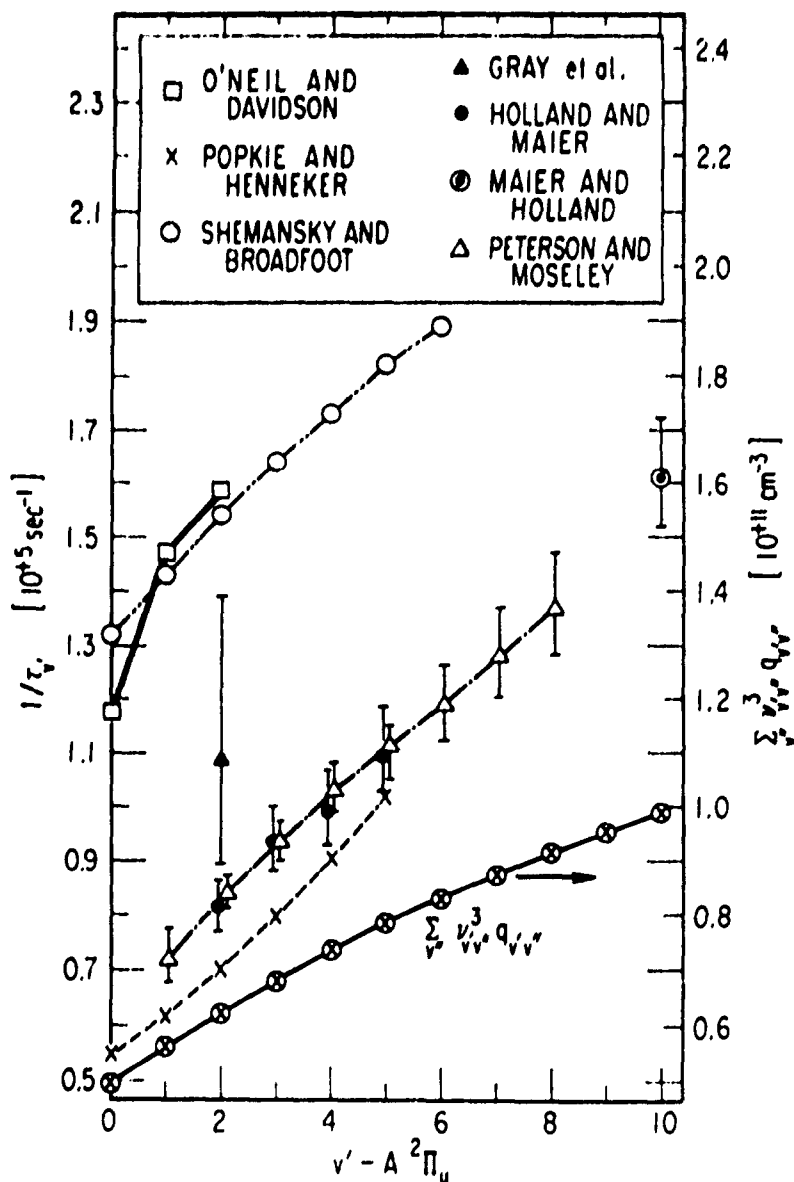


Fig. 2. Inverse of the measured natural lifetimes for the Meinel band system of N_2^+ , as a function of the vibrational quantum number (v'). The data were taken from: □ - O'Neil and Davidson¹¹; x - Popkie and Henneker⁷; ○ - Shemansky and Broadfoot^{10b}; ▲ - Gray et al.^{27a}; ● - Holland and Maier⁴; ⊙ - Maier and Holland⁵; △ - Peterson and Moseley⁶. The lower most curve is a plot (right-hand coordinate) of $\sum_{v''} \nu^3 q_{v'v''}$ as a function of v' .

the ratio of $1/\tau_{v'}$ to $\sum_{v''} \nu_{v'v''}^3 q_{v'v''}$, as a function of v' , as has been done in Fig. 3. As seen from the figure, except for the data of Shemansky and Broadfoot,^{10b} this ratio increases with increasing vibrational quantum number (v'). One might expect that those data whose ratio in Fig. 3 increases with increasing v' would result in a transition moment with a different functional dependence on R from those which generally decrease. This indeed turns out to be the case.

In the analysis of the new lifetime measurements,⁴⁻⁶ the data were divided into two groups. The first group, called Case I, was taken to be the lifetimes for levels $v' = 1-8$ determined by Peterson and Moseley.⁶ The lifetimes for levels $v' = 2-5$ determined by Holland and Maier⁴ are so close to the values assumed in Case I, that their usage in Case I made no substantial difference²⁸ in the results obtained for the coefficients. The second group, called Case II, was formed from Case I by adding the lifetime for $v' = 10$ reported by Maier and Holland.⁵ Cases I and II were analyzed assuming both a linear (two parameter) and a quadratic (three parameter) dependence of the transition moment on internuclear distance [Eq. (13)]. The linear dependence was found to be superior to the quadratic form for both cases on the basis of a combined statistical and physical argument. The statistical consideration is that the confidence limits for the coefficients determined in the quadratic form were at least a factor of five greater than those found for the coefficient in the linear form. This indicates that the linear dependence is a better determined form for the transition moment. The physical reason is based on the fact that both the

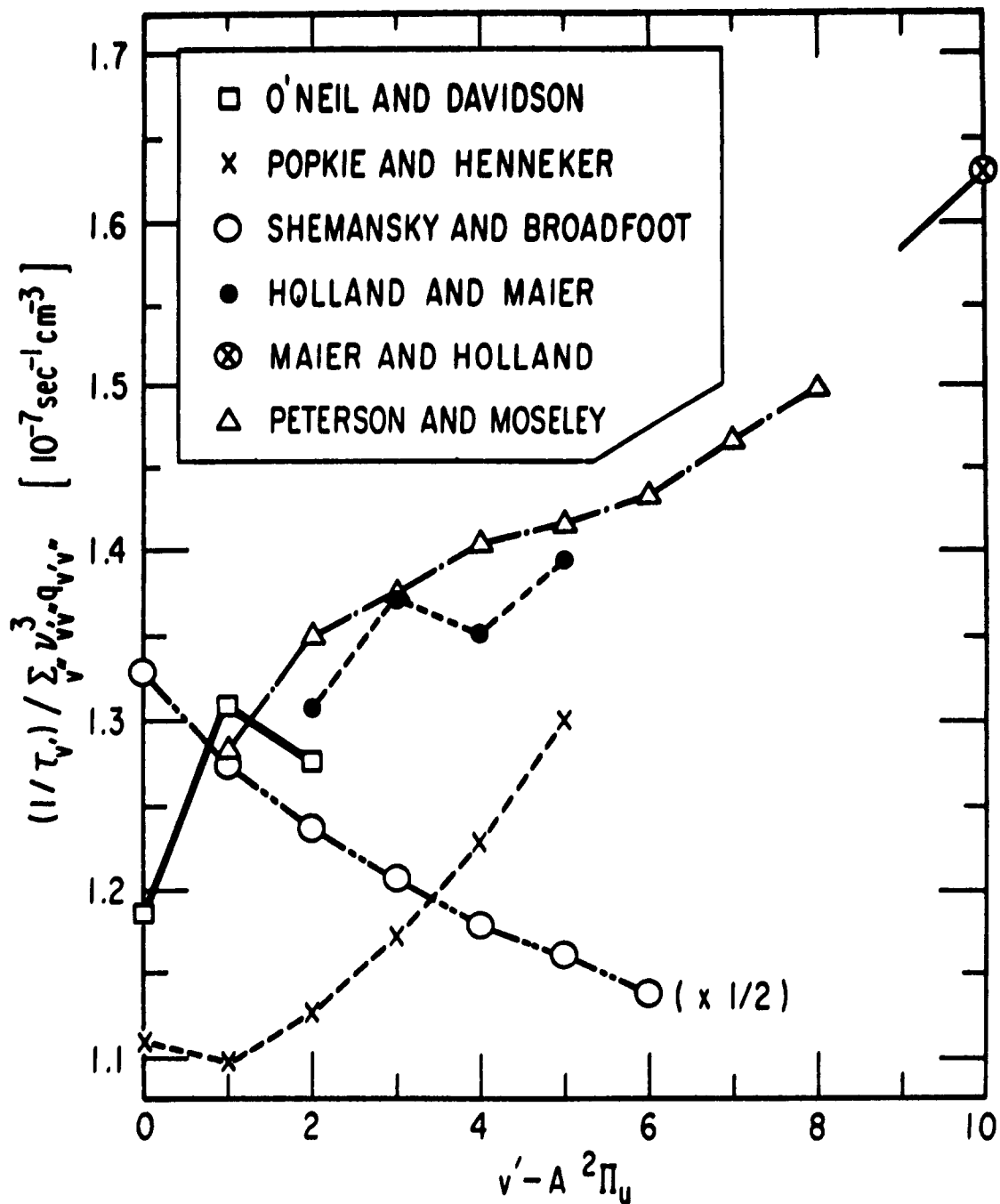


Fig. 3. The ratio of the inverse of the measure lifetimes to the quantity $\sum_{\nu''}^3 \nu_{\nu''}^3 q_{\nu''} \nu_{\nu''}^3$ as a function of ν' . The symbols used for the data are the same as in Fig. 1. The results from the data of Shemansky and Broadfoot^{10b} have been reduced by a factor of two before plotting.

$X^2\Sigma_g^+$ and $A^2\Pi_u$ states dissociate into the same atomic states and therefore the transition moment must vanish at sufficiently large internuclear dependence. The linear dependence monotonically decreases over this range of R-values, but the quadratic form has a minimum near the center of this range and then begins to increase at the larger R-values. These two considerations clearly indicate that the linear form for the transition moment is the better representation of the true moment over this internuclear range.

The coefficients determined for the linear transition moment for both Case I and Case II are given in Table I along with their standard deviation uncertainties. These coefficients were determined using the uncertainties in the lifetime reported for each vibrational level (converted into an uncertainty in the decay constant) as the weights in Eq. (16).

Table I
Optimum Two-Parameter Coefficients in Eq. (13) for Case I and II Data

	a_0 (Debye) [†]	a_1 (Debye Å ⁻¹) [†]
Case I [$v' = 1-8$ (Ref. 6)]	2.412 ± .0417	- 0.9912 ± .0383
Case II [$v' = 1-8$ (Ref. 6), $v' = 10$ (Ref. 5)]	2.675 ± .0365	- 1.231 ± .0336

[†] 1 Debye = 10^{-18} cgsu

The transition moment for Cases I and II is shown in Fig. 4 as the heavy solid lines. The shaded region around the solid line for Case I indicates the uncertainty in the transition moment due to the one standard deviation uncertainty in the coefficients (Table I). The uncertainty range in the transition moment for Case II is similar to that for Case I, but has been omitted from the figure for clarity. The dashed curve labeled PH(T) is the theoretical dipole-length transition moment calculated by Popkie and Henneker⁷ using Hartree-Fock wavefunctions. The shape of the theoretical curve is very similar to that for the present results, but it is a factor of about 2.4 smaller in magnitude. The curve labeled PH(E) is the "experimental" transition moment obtained by Popkie and Henneker⁷ by using the relative intensities for the Meinel system obtained by Stanton and St. John¹³ in a laboratory electron impact excitation experiment, and the preliminary lifetime measurements for levels $v' = 3-5$ by Hollstein et al.¹² for absolute normalization. This transition moment was limited to R-values less than about 1.1 Å because there were not sufficient experimental data available at that time to allow determination of the transition moment at larger R. There does not appear to have been any other experimental or theoretical determination of the internuclear dependence of the transition moment.

If the transition moment depends linearly on R, then the band strength can be written, without approximation, in terms of the Franck-Condon factor

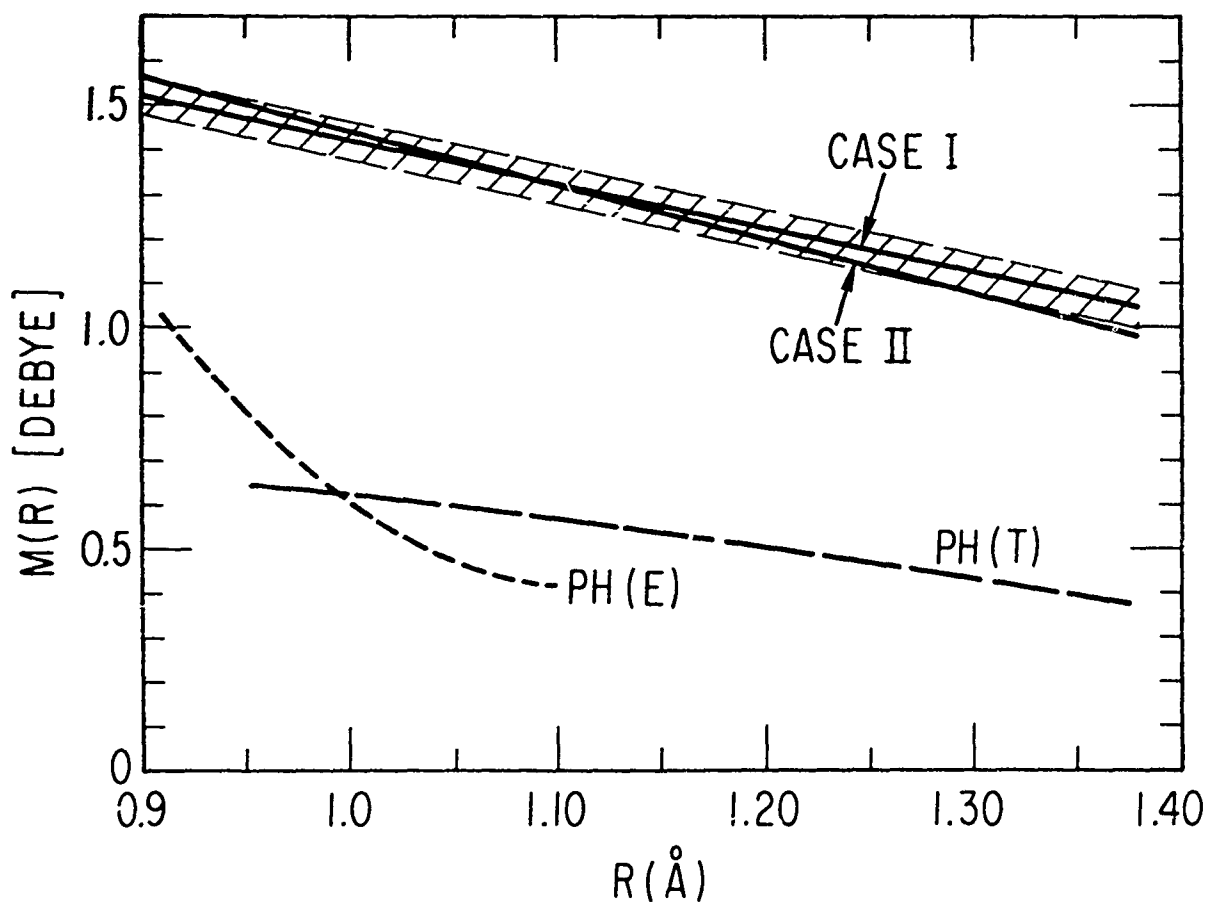


Fig. 4. Dipole-length transition moment (Debye) for the Meinel band system of N_2^+ as a function of the internuclear distance (\AA). The two parameter results obtained for the Case I and Case II data sets are the solid lines. The shaded region around the Case I line denotes the uncertainty in the transition moment due to one standard deviation uncertainties in the coefficients. The curve labeled PH(E) is the dipole-length result obtained by Popkie and Henneker⁷ from earlier data. The curve labeled PH(T) is the theoretical dipole-length moment calculated by Popkie and Henneker⁷ using Hartree-Fock wave functions.

times a function of the r-centroid only. That is, Eq. (14) can, in this case, be rewritten as

$$S_{n'v'}^{n''v''} = \langle v' | v'' \rangle^2 \left[a_0 + a_1 \frac{\langle v' | R | v'' \rangle}{\langle v' | v'' \rangle} \right]^2 \equiv q_{v'v''} R_{el}^2(r_{v'v''}). \quad (23)$$

The quantity R_{el}^2 is sometimes called the electronic band strength although that term is misleading since any dependence of R_{el}^2 on the r-centroid represents a coupling between the vibrational and electronic motions. Except for the work done by Popkie and Henneker,⁷ the previous analyses of experimental Meinel band intensity data have all utilized the r-centroid approximation. Figure 5 compares the present results for R_{el}^2 , as a function of the r-centroid, with the previous determinations. The heavy solid lines represent the two parameter results obtained for Case I and Case II data as labeled and the shaded region around the Case I line represents the one standard deviation uncertainty in R_{el}^2 due to a one standard deviation uncertainty in the parameters a_0 and a_1 . The dashed curve labeled SB is the result obtained recently by Shemansky and Broadfoot^{10b} using relative intensities of the Meinel bands excited by electron impact in a laboratory experiment. They found it necessary to normalize their results to the lifetimes determined by O'Neil and Davidson¹¹ for levels $v' = 0-2$ rather than the more recent beam experiment results of Hollstein et al.¹² in order to insure that their excitation cross section for the Meinel band system did not exceed the total electron-impact ionization cross section for N_2 . Their R_{el}^2 then clearly represents an upper limit to the mag-

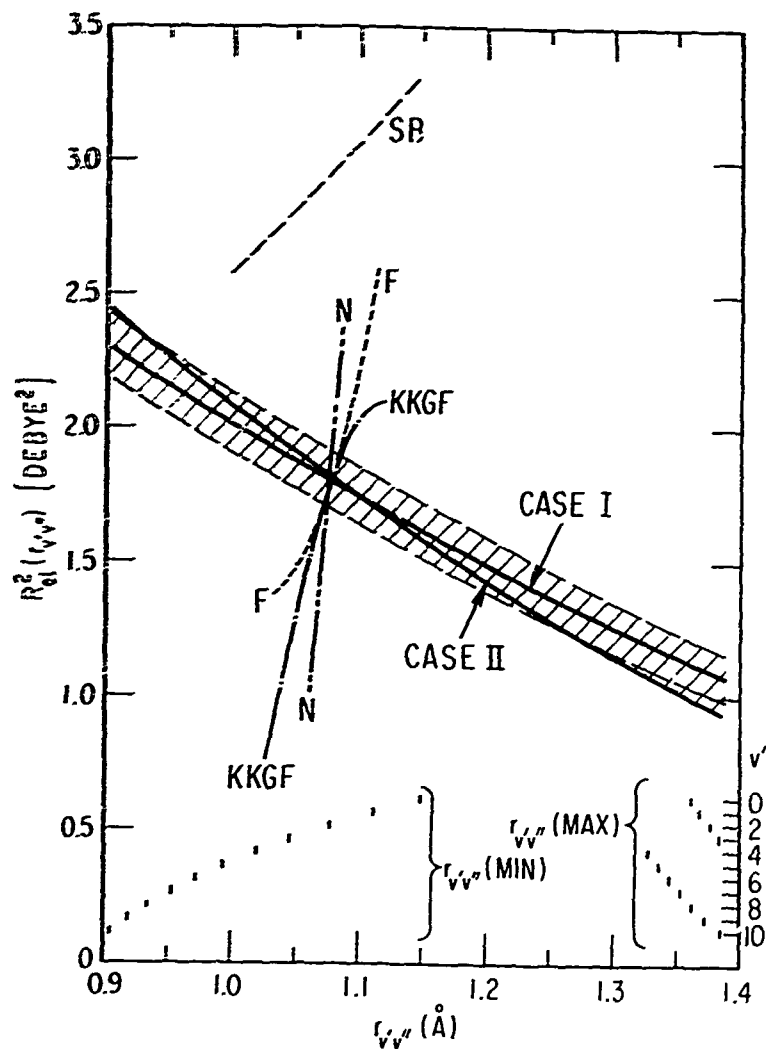


Fig. 5. The "electronic" portion of the band strength, R_{el}^2 in Debye,² as a function of the r -centroid (Å). The solid curves are the two parameter results for the Case I and Case II data sets and the shaded region is the uncertainty due to one standard deviation uncertainties in the parameters. The curves labeled N, F, KKGF and SB are, respectively, Nicholls,^{9a} Fedorova,^{9b} Koppe et al.^{10a} and Shemansky and Broadfoot^{10b}. The short vertical lines at the bottom of the figure are the minimum and maximum values in the range of the r -centroid for fixed v' . See text for discussion of these results.

nitude of the true value. However, it also demonstrates an incorrect dependence on the r-centroid. That is, R_{el}^2 increases with increasing r-centroid while the present results decrease as they should, according to the physical argument stated above. The curves labeled N and F are results obtained from the analysis of auroral relative intensities by Nicholls^{9a} and Fedorova,^{9b} respectively, and have been normalized to the present result at the r-centroid corresponding to the (2, 0) band. The curve labeled KKGF is the laboratory result obtained by Koppe et al.^{10a} from relative intensities of the Meinel bands excited by electron impact in the laboratory. This result has also been normalized to the present result at the (2, 0) band. The R_{el}^2 obtained in these three determinations all increase with increasing r-centroid rather than decrease as in the present results. The short vertical lines at the bottom of Fig. 5 represent the minimum (at the left) and maximum (at the right) values of the r-centroid for each v' and the usefulness of this information will be discussed in the next section.

Some estimates of the quantity R_{el}^2 have also been obtained²⁹ using absolute intensity measurements of the near infrared emissions produced by shock wave through N_2 and air. Krupriyanova et al.^{29b} obtained an estimate of the average value of R_{el}^2 for emissions in the wavelength region 0.9-1.1 μm which agrees fairly well with an upper limit estimate by Wurster.^{29b} However these estimates are somewhat more than a factor of two larger than the present results.

2. Transition Probabilities and Oscillator Strengths

Once the transition moment has been determined, it is straightforward to calculate the band strengths, transition probabilities and oscillator strengths for the Meinel band system of N_2^+ . The transition moment determined obtained using the Case II data were used to generate these quantities which are tabulated in the form of a matrix in Table II. The rows of this matrix are v' and the columns are v'' . Each "element" of this matrix is composed of three numbers. The uppermost is the band oscillator strength, the middle one is the band transition probability, and the lowermost is the band origin wavelength in angstroms. The two columns at the far right are, from left to right, the experimental lifetimes and those calculated from the tabulated transition probabilities. These results are significantly different from previously tabulated results,^{9b,10b} not only in absolute magnitude, but also in relative magnitude for different (v', v'') pairs. The results obtained using the transition moment from the Case I data differ only very slightly from those tabulated here.

The maximum and minimum range of the r-centroid for fixed v' shown near the bottom of Fig. 5 leads to the following useful result. The range of the r-centroid variation for both $v' = 0$ and $v' = 9$ is contained within the ranges for the other v' -levels for which the lifetimes have been measured. As a consequence, the R_{el}^2 determined the v' levels 1-8 and 10, which is an analytic function of the r-centroid, can be interpolated to provide reasonably accurate values for the transition probabilities and oscillator strengths for

Table II
 Oscillator Strengths, Transition Probabilities,
 and Band Origin Wavelengths for the Meinel System of N₂⁺

v'	v''										v ₀ (microns)						
	0	1	2	3	4	5	6	7	8	9	10	11	12	13	Exptl.	Calc.	
0	1.68-3 4.55-4 11086.9	0.71-4 1.36-4 14609.8	1.62-4 1.19-3 21264.9	1.24-5 2.79-1 38500.6	1.91-7 1.70-2 193.4-3												16.57
1	1.40-3 5.53-4 9181.5	1.39-4 3.52-3 11472.4	7.74-4 1.12-4 15210.5	3.04-4 2.02-3 22395.7	3.55-5 6.75-1 41600.3	5.42-7 2.16-2 289.1-3									13.9-1.0	13.88	
2	6.90-4 3.73-4 7852.5	9.87-4 3.67-4 9469.9	4.43-5 1.05-3 11819.6	4.32-4 5.73-3 15851.9	3.66-4 2.19-3 23628.7	6.20-5 9.92-1 43679.6	7.12-7 7.07-3 536.5-3								11.9-0.4	12.04	
3	2.68-4 1.89-4 6873.6	1.01-3 5.17-4 8001.8	3.68-4 1.28-4 9774.0	2.62-4 6.21-3 12.12.2	1.92-4 1.86-3 16540.5	3.49-4 1.86-3 24982.6	0.48-5 1.41-5 567.4-4								10.7-0.4	10.70	
4	9.18-5 8.17-3 6123.0	6.08-4 4.07-4 7063.7	8.85-4 4.26-4 8123.1	4.27-5 1.40-3 10095.4	4.32-4 8.62-3 12772.5	1.84-5 2.05-2 17282.1	2.74-4 1.33-3 26477.2	9.88-5 1.07-2 55519.8							9.7-0.4	9.68	
5	2.94-5 3.20-3 5329.4	2.84-4 2.39-4 6285.2	8.13-4 5.14-4 7263.1	5.42-4 2.46-4 8577.1	1.72-5 5.28-2 10435.5	4.16-4 7.00-3 13263.1	6.38-6 6.51-1 18082.5	1.91-4 8.85-1 28133.0	1.02-4 8.85-1 61996.4						9.1-0.4	8.89	
6	9.07-6 1.19-3 5048.3	1.15-4 1.19-4 5671.0	5.06-4 4.05-4 6455.1	8.04-4 4.80-4 7472.6	2.17-4 9.27-3 8844.8	1.41-4 4.05-3 10795.6	2.95-4 5.18-3 13786.3	9.94-5 5.52-2 18946.9	1.09-4 4.05-2 29972.8	9.52-5 6.49-1 89963.1					8.4-0.5	8.25	
7	2.77-6 4.26-2 4650.7	4.32-5 2.52-4 5174.1	2.56-4 4.05-4 5819.0	6.70-4 5.06-4 6633.2	6.26-4 3.53-4 7692.6	3.41-5 1.37-3 9127.0	2.73-4 7.28-3 11176.9	1.53-4 2.48-3 14344.4	1.25-4 1.05-3 19881.4	4.80-5 1.50-2 38221.6	0.12-5 9.24-1 79957.8				7.6-0.5	7.32	
8	8.43-7 1.51-2 4316.7	1.55-5 2.28-3 4764.0	1.15-4 1.36-4 5305.4	4.20-4 3.93-4 5974.0	7.17-4 5.15-4 6819.9	3.78-4 2.01-4 7923.9	9.06-6 1.90-2 9424.6	3.32-4 6.26-3 11580.9	4.76-5 7.14-2 14940.2	1.69-4 1.29-3 20891.9	1.27-5 3.61-1 34315.0	6.33-5 2.45-1 92818.8			7.3-0.5	7.28	
9	2.59-7 5.31-1 4032.5	5.41-6 9.27-2 4420.1	4.79-5 6.70-3 4882.4	2.23-4 2.51-4 5422.9	5.59-4 4.95-4 6156.4	6.40-4 4.34-4 7016.0	1.61-4 8.05-3 8167.5	7.66-4 2.69-3 9739.0	3.07-4 7.10-3 12009.9	2.42-6 3.33-1 15577.7	1.79-4 1.23-3 21911.1	3.12-7 7.65-1 36893.7	4.50-5 1.24-1 110.0-3		6.91		
10	8.04-8 3.68-2 3787.8	1.88-6 3.10-3 4127.9	1.91-5 3.10-3 4526.3	1.07-4 1.43-4 5006.5	3.52-4 3.76-4 5967.3	6.31-4 5.29-4 6307.3	4.79-4 2.06-4 7222.6	3.17-5 1.49-3 8424.8	1.76-4 5.28-3 10072.3	2.24-4 4.81-3 12467.1	1.91-5 1.20-2 16282.8	1.59-4 9.86-2 23199.1	3.87-6 0.14-0 30822.5	2.88-5 9.31-6 134.0-3	6.2-0.4	6.58	

* Ref. 6 (v' = 1-8), Ref. 8 (v' = 10)

† 1.68-3 = 1.68 x 10⁻³

‡ (v', v'')
 A₂₁² v'' (Å)

transitions from $v'' = 0$ and 9 . These interpolated values are the ones shown in Table II and should be as accurate as the entries involving the other v'' -levels. Since the transition probabilities connecting levels $v'' = 0$ and 9 with all lower v'' -levels are known, they can be summed to provide reasonably accurate life-times for levels $v'' = 0$ and 9 , and the resulting values are given in the right-hand column in Table II. These are useful results because the wavelength region of the fluorescent processes from $v'' = 0$ are in the experimentally difficult near infrared region.

REFERENCES FOR SECTION III

1. A. B. Meinel, *Ap. J.* 112, 562 (1950); *ibid.*, 114 431 (1951).
2. (a) A. Vallance Jones, *Space Science Reviews* 11, 776 (1971). (b) A. Vallance Jones and R. L. Gattinger, "Infrared Spectrum of Aurora," in *The Radiating Atmosphere* (ed. by B. M. McCormac), D. Reidel Publ. Co., Dordrecht-Holland (1971), pp 176-184. (c) R. L. Gattinger and A. Vallance Jones, "The Intensity Ratios of Auroral Emission Features," presented at the XVth General Assembly of the IUGG, Moscow (1971); *Ann. Geophys.* (to be published). (d) A. W. Harrison, *Can. J. Phys.* 47, 599 (1969). (e) *ibid.*, 50, 500 (1972).
3. A. Omholt, *J. Atmos. Terr. Phys.* 10, 320 (1957).
4. R. F. Holland and W. B. Maier, II, *J. Chem. Phys.* 56, 5229 (1972).
5. W. B. Maier II and R. F. Holland, *Bull. Am. Phys. Soc.* 17, 695 (GE8) (1972).
6. J. R. Peterson and J. T. Moseley.
7. H. E. Popkie and W. H. Henneker, *J. Chem. Phys.* 55, 617 (1971).
8. (a) The band strength contains both the electronic and the nuclear vibrational contributions, but not the rotational factors. See J. B. Tatum, *Ap. J. Supp.* 14, 21 (1967). (b) The transition moment is used here to denote the electronic contribution only, which in general depends on the internuclear distance. See eqs. 7 and 9 of reference 7, and reference 8a.

9. (a) R. W. Nicholls, *J. Atmos. Terr. Phys.* 12, 211 (1958). (b) N. I. Fedorova, *Aurora and Airglow* (ed. by V. I. Krasovsky) IGY Program, Section IV, No. 10, NASA TT F-204 (1964), p. 204.
10. (a) V. T. Koppe, A. G. Koral, V. V. Gräsyna, and Ya. M. Fogel', *Opt. Spectrosc.* 24, 440 (1968). (b) E. E. Shemansky and A. L. Broadfoot, *J. Quant. Spectrosc. Radiat. Transfer*, 11, 1385 (1971).
11. R. O'Neil and G. Davidson, U.S. Air Force Cambridge Research Laboratories Report No. AFCRL-67-0277, (1968).
12. M. Hollstein, D. C. Lorents, J. R. Peterson and J. R. Sheridan, *Can. J. Chem.* 47, 1858 (1969).
13. P. N. Stanton and R. M. St. John, *J. Opt. Soc. Am.* 59, 252 (1969).
14. W. H. Henneker and H. E. Popkie, *J. Chem. Phys.* 54, 1763 (1971).
15. A. Schadee, *J. Quant. Spectrosc. Radiat. Transfer* 7, 169 (1967).
16. A. Schadee, *Astron. and Astrophys.* 14, 401 (1971).
17. (a) The atomic unit for energy is the Hartree (27.21165 eV) and that for the line strength is $(ea_0)^2 = 6.460595 \times 10^{-36} \text{ cgsesu}^2 = 6.460595 \text{ Debye}^2$. (b) The constants used here are from B. N. Taylor, W. H. Parker and D. N. Langenberg, *Revs. Mod. Phys.* 41, 375 (1969).
18. See R. W. Nicholls and A. L. Stewart, *Atomic and Molecular Processes* (ed. by D. R. Bates, Academic Press, New York (1962) p. 47, and references therein.

19. (a) J. Drake and R. W. Nicholls, *Chem. Phys. Letters* 3, 457 (1969)
 (b) J. C. McCallum, W. R. Jarman and R. W. Nicholls, *Spectroscopic Report No. 1*, CRESS, York University, Toronto Canada, March 1970.
20. (a) T. C. James, *J. Mol. Spectry* 20, 77 (1966). (b) D. C. Jain and R. C. Sahni, *J. Quant. Spectrosc. Radiat. Transfer* 1, 475 (1967).
 (c) P. H. Krupenie and W. Benesch, *J. Res. Nat. Bur. Stds.* 72A, 495 (1968). (d) D. C. Jain and R. C. Sahni, *Trans. Faraday Soc.* 64, 3169 (1966). (e) H. Klemsdal, *Physica Norvegica* 5, 123 (1971).
21. P. R. Bevington, *Data Reduction and Error Analysis for the Physical Sciences*, (McGraw Hill Book Co., New York (1969), p. 204.
22. *Ibid.*, p. 232.
23. T. R. McCalla, *Introduction to Numerical Methods and Fortran Programming*, (John Wiley and Sons, Inc., 1967), p. 256.
24. R. N. Zare, *J. Chem. Phys.* 40, 1934 (1964); University of California Radiation Laboratory Report No. 10925, (1963).
25. D. Albritton, A. Schmeltakopf and R. N. Zare, *Diatomic Intensity Factors* (Harper and Row, New York, to be published).
26. Ref. 21, p. 153.
27. (a) D. Gray, J. L. Morack and T. D. Roberts, *Physics Letters* 37A, 25 (1971). (b) References 4-7, 10b, 11.
28. By using the Holland and Maier lifetimes for $v' = 2-5$, the leading coefficient a_0 changed by less than 6% and the band strength was within the uncertainty range shown in Fig. 3.

29. (a) W. H. Wurster, *J. Chem. Phys.* 36, 2111 (1962); *J. Quant. Spectrosc. Radiat. Transfer* 3, 355 (1963). (b) Ye. B. Krupriyanova, V. N. Kolesnikov, N. N. Sobolev, *J. Quant. Spectrosc. Radiat. Transfer* 9, 1025 (1969). An English translation of this paper is no longer available from Pergamon Translation Service but one can be obtained from the present author by request.

IV. AUTOIONIZATION

Although autoionization processes in atomic systems have been studied for a number of years,¹ they have just recently been a subject of interest in the case of diatomic molecules. The application of photoelectron spectroscopy² to the study of diatomic molecules has resulted in a number of interesting new problems related to ion production processes in simple molecules. A number of recent studies³ in N_2 using this technique has lead to the postulate that a large fraction of the total ion population is produced by autoionization processes. All of the results of these studies contain pieces of evidence to support this postulate, but the work of Bahr et al.^{3d} and Natalis et al.^{3e} show most clearly how the resulting vibrational population may deviate from that predicted by direct excitation. The problem of dealing with the excitation of each of the many possible Rydberg states and all the possible autoionization paths appears at first to be impossibly complicated. For instance, there are six Rydberg series converging to the B-state and 10 converging to the A-state, that could autoionize into levels of the A-state. However, examination of the possible autoionization decay channels and the energetics involved provides some insight into the specific final states, as can be seen as follows. Those Rydberg states converging to the B-state basically have the configuration

$$1\sigma_g^2 1\sigma_u^2 2\sigma_g^2 2\sigma_u 1\pi_u^4 3\sigma_g^2 Q_{m\lambda} \quad (1)$$

where $Q_{m\lambda}$ denotes the m^{th} Rydberg orbital of angular momentum projection λ . The configuration of the ground state ($X^2\Sigma_g^+$) of the ion is

$$K K K 2\sigma_u^2 1\pi_u^4 3\sigma_g \quad (2)$$

and that for the A $^2\Pi_u$ state is

$$K K K 2\sigma_u^2 1\pi_u^3 3\sigma_g^2 \quad (3)$$

When one of the Rydberg states converging to the B-state autoionizes, the final ion state must be the X or the A state since the Rydberg state is below the ionization limit for the B-state. [Those Rydberg series that converge to the higher vibrational levels of the B-state, and hence above the ionization limit, are very weak because of the Franck-Condon principle.]

By comparing Eqs. (1) - (3), it is evident that the autoionization is a two electron transition involving core relaxation. Furthermore, on examination of the core transition, the final state of the autoionization is found to primarily be the X-state because in that case the core relaxation (or internal conversion) process is dipole-allowed ($3\sigma_g \rightarrow 2\sigma_u$). If the final state were the A-state, it would be dipole-forbidden (but quadrupole allowed) ($1\pi_u \rightarrow 2\sigma_u$). By similar arguments it is noted that those autoionizing Rydberg states converging to the A-state also most likely produce an X-state ion ($3\sigma_g \rightarrow 1\pi_u$). In this case, the B-state is energetically inaccessible for levels of the A-state below $v' = 10$. These arguments lead to the conclusion that most of the autoionization processes will produce ions in various vibrational levels of the X-state. Two important aspects of the argument given above need to be

examined in detail to determine the quantitative details of the autoionization branching ratios. The first is the relative strength of the dipole and quadrupole internal conversion process for the various Rydberg series and the second is the factor or factors that determine the final vibrational population in the X-state. The first aspect can be examined theoretically and some comparisons can be made with the rates known for appropriate transitions in N_2 . There seems to be no direct experimental information available for the N_2^+ states. The recent results from Natalis et al.^{3f} clearly show that an enormous enhancement can be expected for levels of the X-state greater than $v'' = 0$ as a result of the autoionization. This vibrational enhancement, which is a result of the autoionization, is governed by the Franck-Condon factors for transitions connecting the Rydberg state and the X-state. These factors are in turn governed by the shapes of the potential energy curves and their relative internuclear distances. Some preliminary information has been obtained by Bahr et al.^{3d} who found an internuclear distance for the autoionizing Rydberg state that differed from that for the A-state to which it was converging. A good deal more theoretical and experimental work needs to be done in order to answer both questions. As a first step toward understanding the Rydberg states, calculations have been done⁴ on the ground state of N_2 and the three lowest states of N_2^+ . These calculations employ a newly developed generalized valence bond method⁵ which considerably improves on many of the deficiencies that exist in Hartree-Fock calculations. The results of the calculation for the ion states are shown in Fig. 6 as the solid curves. The dashed curves denote the Hartree-Fock

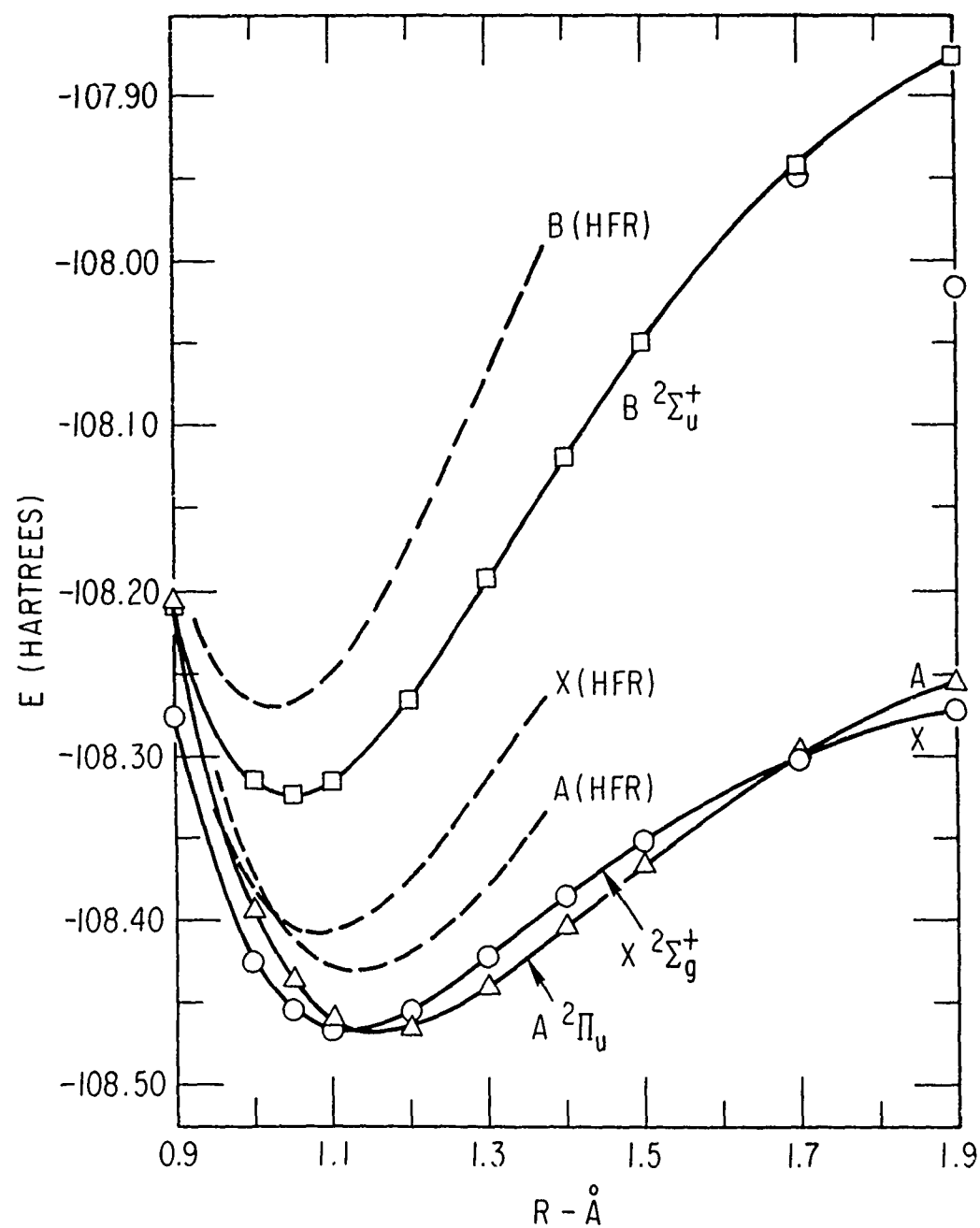


Fig. 6. Potential energy curves for the N_2^+ states as calculated using the GVB method (solid lines) and the Hartree-Fock method (dashed lines).

results of Cade et al.⁶. The ordinate is the total molecular energy in Hartrees (27.21165 eV) and the abscissa is the internuclear distance in Angstroms. Hartree-Fock calculations for the N_2^+ states have two major failings. The first is their improper dissociation behavior, and the second is that they place the A-state below the X-state at the equilibrium separation of the X-state. The new results remove most of these deficiencies and when the proposed configuration interaction calculations are completed, the calculated states are expected to dissociate, and be ordered, properly. These theoretical calculations of the ion states will then serve as the basis for examining the autoionization details mentioned above. With at least a basic understanding of the autoionization from Rydberg states, it is believed that the more complicated processes of interest such as resonance fluorescence and dielectronic recombination can be examined. The understanding of these processes requires that two additional problems be solved. That is, the quantitative rates of excitation to the Rydberg states must be known, and the competition between autoionization and radiative decay of the Rydberg state must be examined. The theoretical work reported here also serves as the foundation for this work which will hopefully be completed in the near future.

REFERENCES FOR SECTION IV

1. A. Temkin (ed.), Autoionization, (Mono Book Corp., Baltimore, 1966).
2. A partial review of the work being done is found in Phil. Trans. Roy. Soc. Lond. A268, pp. 1-200 (1970). See also Reference 3 below.
- 3(a). J. E. Collin and P. Natalis, Int. J. of Mass Spectrometry and Ion Physics 2, 231 (1969). (b) J. Berkowitz and W. A. Chaupka, J. Chem. Phys. 51, 2341 (1969). (c) T. A. Carlson, Chem. Phys. Letters 9, 23 (1971). (d) J. L. Bahr, A. J. Blake, J. H. Carver, J. L. Garner and V. Kumar, J. Quant. Spec. Radiat. Transfer 11, 1839 (1971). (e) T. A. Carlson and A. E. Jones, J. Chem. Phys. 55, 4913 (1971). (f) P. Natalis, J. Delwiche and J. E. Collin, Chem. Phys. Letters 13, 491 (1972).
4. These calculations have been done in collaboration with Dr. Thom Dunning of the California Institute of Technology, and using computer programs developed by he and others from Cal Tech.
5. W. A. Goddard, III, Phys. Rev. 157, 81 (1967).
6. P. E. Cade, K. D. Sales and A. C. Wahl, J. Chem. Phys. 44, 1973 (1966).

Preceding page blank

V. QUENCHING OF THE $B^2\Sigma_u^+$ AND $A^2\Pi_u$ STATES

In developing a model for the quenching of the A-state, it is worthwhile examining the quenching of the B-state because of possible similarities. The lifetimes of the B-state are reviewed first because the reported quenching rates depend on the value of the lifetime used.

A. Lifetimes for the $B^2\Sigma_u^+$ State

The lifetime of the zeroth vibrational level of the B-state has been measured many times¹⁻¹² because of its importance in atmospheric processes and the relative ease of measurement. The older measurements for the lifetime of $v' = 0$ generally differ by somewhat more than ten percent, but the more recent measurements appear to have converged to a value of about 59.0 ns. On the other hand, the lifetime of level $v' = 1$ has been reported only three times and the values reported differ in their magnitudes relative to that for $v' = 0$. Those lifetimes which have been found in the open literature or technical reports are summarized in Table III.

Many different experimental techniques have been employed to populate the $B^2\Sigma_u^+$ state of N_2^+ and all but two of the measurements reported use the measured time dependence of the decay of the fluorescence to determine the lifetimes. Both Fink and Welge,¹¹ and Hesser⁵ used the phase shift method which measures the lifetime directly. To produce a population of the B-state, Jeunehomme⁷ used an RF discharge, and Fowler and Holzberlein⁸ used a Holzberlein gas discharge. Buttrey and McChesney³ used a shock wave, and Nichols and Wilson⁴ employed a high-energy pulsed-proton beam to excite the

Table III. Lifetimes for $B^2\Sigma_u^+$ of N_2^+

(nsec)		Reference
$v' = 0$	$v' = 1$	
58.6 ± 5.0	62.0 ± 5.0	1
59.2 ± 4.0	58.5 ± 4.0	2
62.0 ± 18.6		3
65.9 ± 1.0		4
59.2 ± 6.0		5
66.6 ± 1.3		6
71.5 ± 4.0	75.8 ± 4.0^b	7 ^a
82.0 ± 8.0		8
40.0 ± 20.0^c		9
65.0 ± 2.0		10
60.0 ± 4.0^d		11
65.8 ± 3.5		12

a) Also contains rough lifetime estimates for $v' = 2, 3$ and 4 .

b) Uncertainty assumed to be the same as for $v' = 0$.

c) Value taken from Reference 1.

d) Obtained by considering only electron energies greater than 70 eV.

radiation. Johnson and Fowler,² Sebacher,¹⁰ Bennett and Dalby,¹² Hesser,⁵ and Fink and Welge¹¹ all employed a pulsed electron beam for excitation. and Desesquelles et al.⁶ used static target gases to excite accelerated N_2^+ ions into the B-state.

Based on the most recent measurements, a value of about 59.0 ± 2 nsec appears to be the best value for the lifetime of the $v' = 0$ level of the B-state. This value is about ten percent smaller than the previously accepted value¹² of 65.8 ± 3.5 nsec.

The situation for $v' = 1$ is not as good as for $v' = 0$. Head¹ reported a lifetime which is longer than that for $v' = 0$, while Johnson and Fowler² and also Jeunehomme⁷ reported a value that is smaller than for $v' = 0$. Some additional information on this point can be obtained by using the recent results of Brown and Landshoff¹³ who reported an improved determination of the electronic transition moment for the First Negative system. If their dependence is used to calculate the transition probabilities, the lifetime for $v' = 1$ is found to be slightly smaller than that for $v' = 0$. The functional dependence determined by Brown and Landshoff is used to calculate the transition probabilities for the First Negative system in which all the values have been adjusted to give a lifetime of 59.0 nsec for the $v' = 0$ level. The obtained transition probabilities are given in Table IV. The resulting lifetimes for the B-state are given in the last column of Table IV.

Table IV. Transition Probabilities for the First Negative System of N_2^+

v'	v''	0	1	2	3	4	5	6	7	8	9	10	$\bar{\nu}$ (cm ⁻¹)
0	0	1.18 +7 3911.4	4.05 +6 4275.1	9.24 +5 4700.1	1.74 +5 5224.8	2.80 +4 5860.5	4.24 +3 6657.6	4.93 +2 7685.8	4.51 +1 9061.9				59.0
1	0	6.17 +6 3579.4	4.09 +6 3881.6	4.55 +6 4233.6	1.78 +6 4748.8	4.71 +5 5145.4	1.01 +5 5749.8	1.86 +4 6501.0	2.82 +3 7459.0	3.31 +2 8723.1	3.36 +1 10463.4		58.2
2	0	9.84 +5 3305.0	8.32 +6 3561.0	9.68 +5 3855.1	3.72 +6 4196.3	2.28 +6 4596.8	8.12 +5 5073.2	2.18 +5 5649.1	4.89 +4 6358.8	9.15 +3 7254.4	9.15 +3 8419.1	1.29 +3 9994.4	57.6
3	0	4.65 +4 3025.4	2.29 +6 3295.9	8.51 +6 3546.2	5.80 +4 3832.9	2.56 +6 4164.3	2.40 +6 4551.6	1.11 +6 5009.8	3.64 +5 5960.1	9.62 +4 6232.9	2.15 +4 7073.7	3.50 +3 8153.2	57.3
4	0	1.49 +2 2880.9	1.32 +5 3073.5	3.54 +6 3290.1	7.95 +6 3535.4	1.02 +5 3815.5	1.54 +6 4138.1	2.24 +6 4513.4	1.30 +6 4955.2	5.09 +5 5482.7	1.56 +5 6122.9	4.01 +4 6915.7	57.1

B. Quenching Rates for the B-State

A thorough review of the quenching rates for $v' = 0$ of the B-state is given by Mitchell¹⁸ so the discussion here will focus on the rates obtained using the improved lifetimes, the work done since the publication of Mitchell's paper, and the quenching rate for $v' = 1$. The hope of this procedure is that some information will be gained that can be applied toward understanding the quenching of the A-state.

Table V summarizes the quenching rates of $v' = 0$ and 1 of the B-state by four different gases. These quenching rates have been all referenced to a lifetime of 59.0 ns for both levels even though the lifetime for $v' = 1$ is probably slightly shorter (see Table III). Johnson and Fowler,¹⁷ and Mackay and March¹⁹ used a pulsed electron source, Comes and Speier^{14,20} used a pulsed He I (584 Å) photon source, Smelley¹⁵ and Walters¹⁶ used a 1.5 MeV proton beam, and Mitchell¹⁸ used a soft x-ray source, to excite the N_2^+ B-state. The quenching rates were then determined by examining the pressure dependence of the intensity in the First Negative system.

The value for the quenching rate of $v' = 0$ by N_2 appears to be reasonably well determined at about $5.0 \pm 1.0 \times 10^{-10} \text{ cm}^3/\text{sec}$. For quenching of $v' = 0$ by O_2 , a rate of $6.9 \pm 1.5 \times 10^{-10} \text{ cm}^3/\text{sec}$ is also consistent with the experimental findings. The quenching values for $v' = 1$ are less certain however. Both Comes and Speier,²⁰ and Johnson and Fowler¹⁷ found $v' = 1$ to be quenched more rapidly than $v' = 0$, and by about the same relative amount. Mackay and March,¹⁹ however, found $v' = 1$ to be less rapidly quenched. This is an important point for the Meinel study because the result of the quenching of the B-state

Table V. Quenching Rates for $B^2\Sigma_u^+$ (10^{-10} cm³/sec)

	<u>N₂</u>	<u>O₂</u>	<u>NO</u>	<u>CO₂</u>	<u>Reference</u>
(v' = 0)	5.4 ± 1.0				14
	2.44 ± .32	6.36 ± .89			15
	3.60 ± 1.0			9.70 ± 2.2	16
	2.70 ± 1.3				17
	5.05 ± .9	8.21			18
	(6.1-7.8) ± 1.7		8.6 ± 1.7		19
		6.87 ± 1.5			20
(v' = 1)					
	13.2 ± 2.3				14
	4.8 ± 1.3				17
	4.9 ± 1.9		3.0 1.3		19
		14.6 3.0			20

is postulated by Comes and Speier²⁰ to be the A-state of N_2^+ . Their model, and hence the formation of the A-state as a final product of the quenching, requires the rate to increase with increasing v^1 . Unfortunately, it has not yet been possible to evaluate their model quantitatively but the available experimental evidence does seem to favor an increase in the quenching rate with increasing v^1 . This is an interesting mode for population of the A-state in atmospheric processes and would become important at altitudes below about 70-90 km. A rate of $13.2 \pm 2.3 \times 10^{-10} \text{ cm}^3/\text{sec}$ appears to be a good value for the quenching of $v^1 = 1$ by N_2 , and $14.6 \pm 3.0 \times 10^{-10} \text{ cm}^3/\text{sec}$ for quenching by O_2 .

Some information on the temperature dependence of the quenching of $v^1 = 0$ has been obtained by Flagan and Appleton²¹ through the analysis of shock tube data. Their lowest temperature point was 5000°K , but the extrapolation of their rate to 300°K results in a rate that is two orders of magnitude too large. Inspection of their Fig. 4 and their temperature dependence indicates, however, that the 300°K rate could easily be combined with their high temperature results to give an overall temperature dependence that is consistent with their interpretation.

For completeness, the relationship between the quenching constant, that appears in the fluorescence efficiency, and the quenching rate is given here as¹⁸

$$K(\text{torr}^{-1}) = a(\text{cm}^3/\text{sec}) \cdot [3.22 \times 10^{16} \text{ cm}^3 \cdot \text{torr}^{-1} \cdot \tau_{v^1}(\text{sec})] .$$

The fluorescence efficiency, at any pressure $P(\text{torr})$, is then given by

$$\eta(P) = \frac{\eta_0}{(1 + KP)}$$

The quenching results summarized in Table V can then be used with the η_0 values of Mitchell,¹⁸ to estimate the fluorescence efficiency of the First Negative of N_2^+ in the atmosphere.

C. Quenching Rates for the A-State

The quenching processes for the A-state of N_2^+ have not been as extensively studied as those for the B-state because of the experimental difficulties associated with its long lifetimes. Sheridan et al.²² estimated the quenching rate, by N_2 , for the $v' = 2$ level to be $1.0 \times 10^{-9} \text{ cm}^3 \text{ sec}^{-1}$, based on a lifetime for that level of $3 \mu\text{sec}$. If the new lifetime of about $12 \mu\text{sec}$ is used (Section III) the quenching rate they measured becomes about $3.8 \times 10^{-10} \text{ cm}^3/\text{sec}$. The extensive measurements of O'Neil and Davidson²³ on the fluorescence efficiency of air excited by high energy electrons resulted in an estimate of the N_2 quenching rate for the lower levels of the Meinel bands of $3.7 \times 10^{-10} \text{ cm}^3/\text{sec}$. This is surprisingly close to the corrected result due to Sheridan et al. Mitchell²⁴ has also independently estimated the N_2 quenching rate for the lower levels of the Meinel system to be about $4.0 \times 10^{-10} \text{ cm}^3/\text{sec}$. Simpson and McConkey²⁵ measured the ratio of the N_2 quenching cross section to the Einstein transition probability for the Meinel bands excited by 80 and 120 eV electrons. If the transition probabilities reported in Section III are used to extract the quenching rates from their ratios, one obtains the results summarized in Table VI.

The quenching rate obtained from the data of Simpson and McConkey for levels $v' = 2$ and 3 are thus very similar to that rate found by Sheridan et al., O'Neil and Davidson, and Mitchell. Based on these independent experimental determinations of the quenching rate for $v' = 2$, a reasonable value for the quenching of this level $N_2 (X^1 \Sigma_g^+)$ is

Table VI

Quenching rates for the Meinel bands obtained from data of Simpson and McConkey²⁵ and transition probabilities of Section III.

(v', v'')	$\alpha (10^{-10} \text{ cm}^3/\text{sec})$	
	80 eV	120 eV
(2, 0)	3.8	3.0
(3, 0)	4.3	4.2
(4, 0)	5.1	-
(4, 1)	7.1	4.4
(5, 2)	18.6	13.4

$$4.0 \pm .5 \times 10^{-10} \text{ cm}^3/\text{sec}$$

It is noted that this value is nearly the same as that found for the analogous quenching of $v' = 0$ of the B-state. One might expect this to be more-or-less the case for non-resonance quenching because the A and B states are fairly similar. However, the vibrational dependence of the quenching ratio is still uncertain since the only measurements that are available are those by Simpson and McConkey²⁵ for $v' = 2-5$. The source of the energy dependence of the quenching rate, seen by O'Neil and Davidson²³ and Simpson and McConkey,²⁵ is not yet understood, nor are the details (e.g., final states, etc.) of the quenching process itself. The research presently being conducted at Utah State University should provide some of the information needed to understand the quenching processes.

Until more experimental information becomes available and/or a theoretical model is developed to explain the quenching, reasonable estimates for the vibrational dependence of the quenching would be that found by Comes and Speier²⁰ for the quenching of the A $^2\Pi$ state of CO^+ by CO. This process is exactly analogous to the quenching of the A-state of N_2^+ by N_2 , and for non-resonant quenching, they should provide reasonably good values. These values are given in Table VII. One notes that the quenching rates for the lower levels of the CO^+ (A) state are indeed very similar to those found for the same levels of the N_2^+ (A)-state. Although it is believed that the increase in the quenching rate

Table VII. Quenching²⁰ of CO⁺ (A²Π) by CO

v'	$(10^{-10} \text{ cm}^3/\text{sec})$
0	3.2 ± 1.9
1	5.5 ± 0.9
2	7.0 ± 1.2
3	8.0 ± 0.9
4	8.0 ± 1.4
5	11.9 ± 1.5
6	12.0 ± 2.7
7	14.7 ± 2.5
8	15.7 ± 2.7

as a function of v' shown in Table VII is probably reasonable for the quenching of N₂⁺ (A) by N₂, some caution should accompany its application for the higher N₂⁺ (A)-levels because of the possibility of resonance quenching effects. Similar resonant effects are not expected for CO⁺ (A) because of the somewhat different shapes for the potential energy curves of CO⁺ from those for N₂⁺.

REFERENCES FOR SECTION V

1. C. E. Head, *Physics Letters* 34A, 92 (1971).
2. A. W. Johnson and R. G. Fowler, *J. Chem. Phys.* 53, 65 (1970).
3. D. E. Buttrey and H. R. McChesney, Tech. Report No. AFWL-TR-69-29, Kirtland Air Force Base, New Mexico (1969).
4. L. L. Nichols and W. E. Wilson, *App. Optics* 7, 167 (1968).
5. J. E. Hesser, *J. Chem. Phys.* 48, 2518 (1968).
6. J. Desesquelles, M. Dufay and M. C. Poulizac, *Physics Letters*, 27A, 96 (1968).
7. M. Jeunehomme, *J. Chem. Phys.* 44, 2672 (1966).
8. R. G. Fowler and T. M. Holzberlein, *J. Chem. Phys.* 45, 1123 (1966).
9. H. Anton, *Ann. Physik* 18, 178 (1966).
10. D. I. Sebacher, *J. Chem. Phys.* 42, 1368 (1965).
11. Von E. Fink and K. H. Welge, *Z. Naturforschg.* 19a, 1193 (1964).
12. R. G. Bennett and F. W. Dalby, *J. Chem. Phys.* 31, 434 (1959).
13. W. A. Brown and R. K. Landshoff, *J. Quant. Spect. Rad. Transfer* 11, 1143 (1971).
14. E. J. Comes and F. Speier, *Chem. Phys. Letters* 4, 13 (1969).
15. A. R. Smelley, (thesis) Naval Postgraduate School (1969).
16. R. F. Walters, (thesis) Naval Postgraduate School (1970).
17. A. W. Johnson and R. G. Fowler, *J. Chem. Phys.* 53, 65 (1970).
18. K. B. Mitchell, *J. Chem. Phys.* 53, 1795 (1970).

19. G. I. Mackay and R. E. March, *Can. J. Chem.* 49, 1268 (1971).
20. F. J. Comes and F. Speier, *Z. Naturforsch.* 26A, 1998 (1971).
21. R. C. Flagan and J. P. Appleton, *J. Chem. Phys.* 56, 1163 (1972).
22. W. F. Sheridan, O. Oldenberg and N. P. Carleton, in Atomic Collision Processes, edited by M. R. C. McDowell, (North-Holland Publishing Co., Amsterdam (1964), p. 440.
23. R. O'Neil and G. Davidson, AFCRL-67-0277, ASE-1602, American Science and Engineering, Inc., Cambridge, Mass. (1968).
24. K. B. Mitchell, J-10 Division, Los Alamos Scientific Laboratory, Presentation made at the ARPA Prime Argus Meeting, January 1972. (unpublished).
25. F. R. Simpson and J. W. McConkey, *Planet. Space. Sci.* 17, 1941 (1969).

VI. EXTRACTION OF LIFE TIMES FROM FLUORESCENT DECAY DATA

A. INTRODUCTION

Knowledge of the natural (radiative) lifetimes of excited states of atoms and molecules is important in many areas of basic and applied science. From analysis of lifetime data it is possible, in most cases, to extract the band strengths which characterize completely the absorption and emission properties of the isolated atom or molecule. For example, it is these properties which are essential for the analysis of a potential laser system and for the interpretation of emissions observed from the upper atmosphere. One of the most reliable and often used experimental techniques for obtaining the radiative lifetimes is the measurement of emission decay curves. The method described here was developed to analyze emission decay curves which contained contributions from two or more excited states. The model assumed in fitting the data is described in Section B. The structure of the program and interpretation of the results are treated in Section C. Examples of the use of this method in the analysis of NI, N₂ and N₂⁺ emission decay curves are given in Section D.

The primary reason for developing this computer program was to provide Drs. Bill Pendleton, Jr. and Larry Weaver of Utah State University (who are studying excitation and quenching processes in the Meinel Band system) with a means to check their data analysis which does not utilize the program FRANTIC.

B. METHOD

1. Theory

An excellent review of the different techniques used to extract natural lifetimes from decay curves has been given by Bennett et al.¹. Following development given there, the instantaneous number of photons detected from the excited state is represented by

$$N(t) = \sum_{j=1}^P C_j e^{-A_j t} \quad (1)$$

where N is the instantaneous number of photons (counts), P is the number of components present, C_j and A_j are respectively the amplitude (number of "atoms" in the excited state j) and the decay rate of the j^{th} component.

Instead of measuring the instantaneous decay, each channel actually detects the decay in a time interval Δt_i corresponding to channel i . Equation (1) can be integrated from t_i to $t_i + \Delta t_i$ to give

$$N_i \Delta t_i = \sum_{j=1}^P C_j e^{-A_j t_i} \left(\frac{1 - e^{-A_j \Delta t_i}}{A_j} \right) \quad (2)$$

where N_i is the number of counts collected in channel i (t_i to $t_i + \Delta t_i$). Dividing both sides of Eq. (2) by Δt_i , one arrives at the functional form to which the basic data (N_i) is to be fit

$$N_i = \sum_{j=1}^P C_j e^{-A_j t_i} \left(\frac{1 - e^{-A_j \Delta t_i}}{A_j \Delta t_i} \right) \quad (3)$$

The unknown parameters, C_j and A_j , are determined by a least squares fitting procedure to the experimental data. Although the parameters C_j are linear in Eq (3), the A_j are nonlinear which makes the actual fitting procedure considerably more difficult. A description of the computer program TAUFIT, which determines the parameters C_j and A_j from experimental data, is given in the next section.

2. Program Description

The program TAUFIT has two capabilities which results in a very flexible fitting routine. The first is the nonlinear least square subroutine called GAUSAUS,² which forms the heart of the program. The second is the CDC NAMELIST³ option, which allows one to read and write without formatting, and provides considerable flexibility in data manipulation. The options for data handling, weighting and smoothing are controlled via input data through the use of NAMELIST.

Smoothing :

N data-smoothings are performed by setting NSMOOTH = N, where N is an integer. A 1-2-1 triangular smoothing is employed and the program is constructed such that smoothing does not destroy the input data. This allows other manipulations of the data to be performed without rerunning the data set.

Weighting :

Weighting is accomplished by setting IWEIGHT = 2 or IWEIGHT = 3. When IWEIGHT = 3, the program fits the data first without weighting and then refits the original data using the residuals from the first attempt as weights for the second try. When IWEIGHT = 2, the data itself is used

for weighting, i.e., $w_i = \frac{1}{\sigma_i^2} = \frac{1}{N_i}$.

The program parameters and options are given in the program listing in the Appendix. Note that the variable format, IMAT, and the NAMELIST options allow for very flexible inputting of data; e.g., the variable format, IMAT, can dictate that any number of data cards and fields be skipped before the desired data points are read-in. The number of data points may exceed those skipped and read-in since NAMELIST will skip them looking for the proper declarations. This allows one to keep data decks intact and still only fit that selected portion of data sequence corresponding to decay.

It is emphasized that although the NAMELIST option is convenient, it is not essential in using this program. The main routine can be easily modified to use the conventional input procedure without altering the usefulness of the program.

C. USAGE AND INTERPRETATION

1. Data Set Structure

Data Card(s)

1. and 2. Title cards (ITITLE)
3. Variable format (IMAT) card for reading multichannel analyzer data.
4. Number of data points (NOB) to be used during the fitting process.

Multichannel analyzer data (OBS)

NAMELIST program options.

- a. Each program option section is preceded by a \$OPTIONS card, and followed by a \$ card. In both cases the \$ must be in column 1. See the appendix (card section B) for those items which are included in the options section. NOTE: Only those options

actually specified are affected, and others remain as they were or assume their default values.

- b. As many option sections as deemed necessary may be used
Any number of data sets may be submitted.

2. NAMelist Options

Aside from reading multichannel analyzer data, all program parameters are handled through NAMelist. These parameters include:

LL, P, UL: Arrays specifying the lower limits, initial guesses and upper limits, respectively, for the coefficients, lifetimes and background components. When specifying these parameters, all the coefficients are specified first, then the lifetimes followed by the background components. These parameters must be specified initially as they have no default values. They need only change when the number of lifetimes change, or multichannel analyzer data warrants it.

NTAUS: An integer specifying the number of lifetimes to be used in the fit. NTAUS must be specified initially as there is no default value.

NBKG: An integer specifying the type of background (polynomial) used. The initial default value is no background, NBKG = 0, but any assigned value stays in effect until changed.

NPROB: User problem number. The default value is one. It has no affect on program operation; it is merely for user conveniences.

NSMOOTH: An integer specifying the number of times the data is to be smoothed. No smoothing is the default condition, and smoothing must be specified in each options section, if desired.

IWEIGHT: An integer specifying the type of weighting to be used in the fit. No weighting is the default condition, and weighting must be specified in each options section, if desired.

TO: Channel relative to the first channel in the multichannel analyzer data at which the fit is to start. For example, if three data cards were skipped when reading data, and there were ten channels per card, $TO = 31.0$. The initial default value is $TO = 1.0$.

DT: Dwell time per channel. Must be initialized by the user.

DEND: A logical variable specifying that the last options group for a particular data set has been encountered, i.e., when $DEND = TRUE$. After performing the various tasks dictated by the other namelist parameters, the program will look for a new data set. Of course the default value is $DEND = FALSE$.

3. Results

a. Output

The raw data, model and residuals are listed with appropriate titles. The initial parameter guesses along with their ranges are listed with the data. The final parameters values and their confidence limits are listed with each model. Also listed are RMS and notes concerning weighting and smoothing. For each model used, the program plots the raw data and the

best fit on the same plot.

b. Interpretation and Usage

As with all nonlinear least-squares programs, a great deal of subjectivity is required by the user. In TAUFIT, reasonable initial guesses must be made for the parameters, especially for the linear coefficients. If the sum of the coefficients is too large or too small, say ten times $N(t = 0)$ or 0.1 times $N(t = 0)$, respectively, the program will not be able to reduce the sum-of-squares, and hence will not improve the parameters.⁴ The parameter limits should not be overly tight, as one or more parameters may be constrained by a range limit resulting in a poor fit.

In dealing with data for which the lifetimes, or number of lifetimes, are unknown, it is suggested that the following procedure be used. First, fit the data with at least one fewer lifetimes than suspected. Then increase the number of lifetimes by one in each subsequent fit. For each fit, compare the RMS deviations and parameter confidence limits. One might expect that the lowest RMS would accompany the tightest confidence limits. In practice this is often not the case. When the number of parameters is over or under specified, the confidence limits are usually poorer. On the otherhand, the more parameters specified, the lower the RMS. Hence, the subjective aspect of fitting. Generally, one should question confidence limits which are greater than 50 percent of the parameter value, unless its contribution to the total fit is small.

The plots produced are usually useful in determining when a good fit has been obtained for a given data set. When the fit is poor, it is usually immediately obvious from inspection of the plots.

D. EXAMPLES

1. The 1200 Å Doublet of Ni ($3^4P - 2^4S$)

This computer program was tested using fluorescent decay data containing two components with known lifetimes. These data were kindly provided by Dr. George Lawrence of the University of Colorado who has analyzed these data using the program FRANTIC. Table VIII shows a comparison of the lifetimes obtained with this program and those obtained by Lawrence using FRANTIC.

Table VIII. Fluorescent Decay of the 1200 Å Doublet of Ni

Data Set	Lifetime (nsec) Components			
	Present		Lawrence (FRANTIC)	
	τ_1	τ_2	τ_1	τ_2
A	$2.51 \pm .07$	54.4 ± 2.0	$2.51 \pm .05$	$53.5 \pm .48$
B	$2.48 \pm .08$	53.0 ± 2.3	$2.47 \pm .05$	54.0 ± 1.9
C	$2.29 \pm .07$	54.6 ± 2.0	$2.31 \pm .05$	$54.8 \pm .45$

There is excellent agreement between the results obtained by the two independent methods. The uncertainties quoted in the present results are confidence limits based on one standard deviation. The reason that the uncertainties quoted by Lawrence are smaller than the present values is not clear, but probably reflects a slightly different treatment of the statistics in his case.

Figure 7 shows the raw data (points) and resulting fit to the data (solid line) for each of the three cases. In general the fits are excellent.

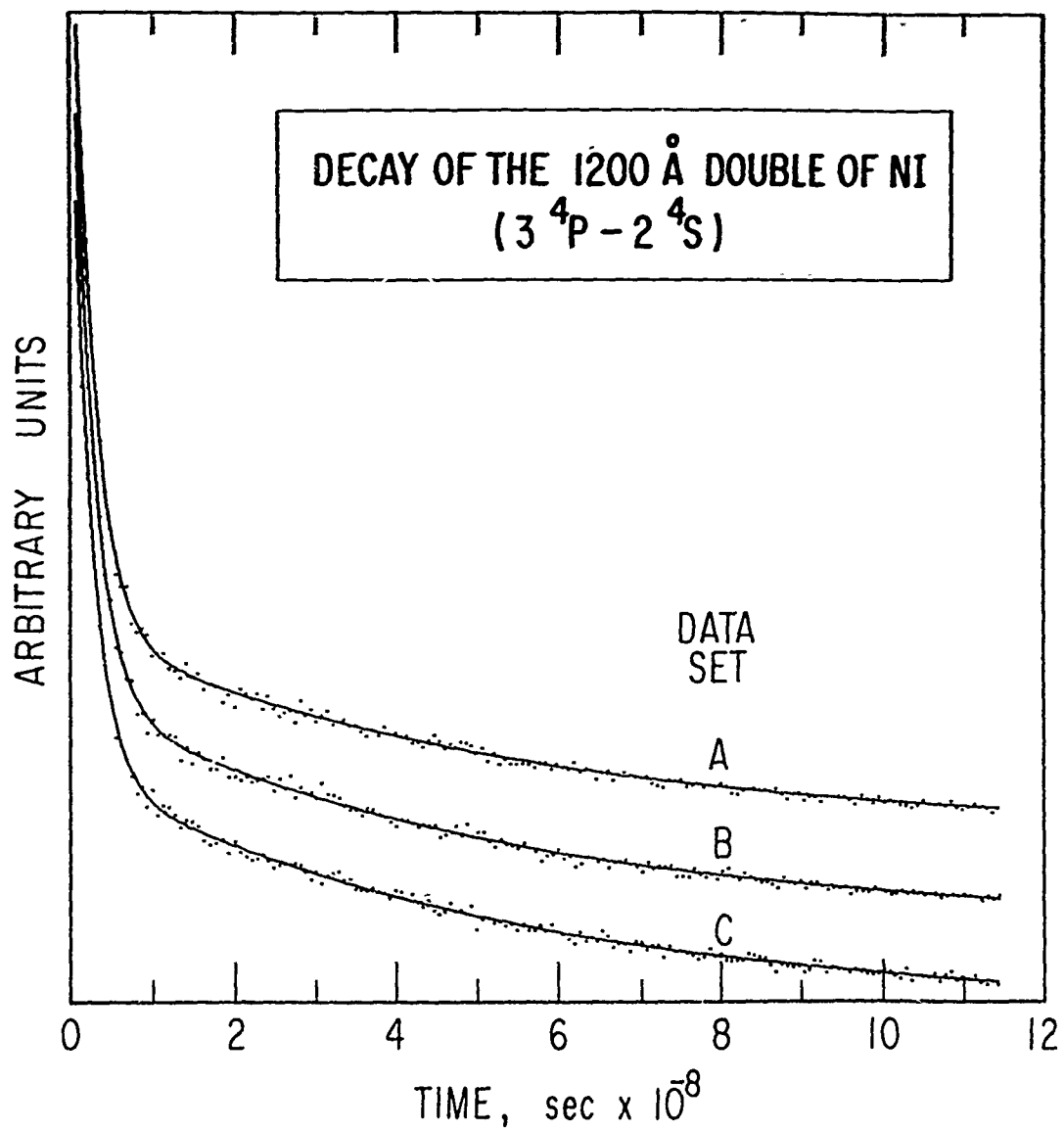


Fig. 7. Fluorescent decay data and the best fit to them for the NI doublet at 1200 Å.

2. The N₂ (3,1) (9,6) First-Positive Bands

Dr. W. Pendleton provided fluorescent decay data for the (3,1) band of the First-Positive system which also contains a contribution from the (9,6) band. The input data, which has been smoothed once, and the resulting best fit are shown in Figure 8. The result obtained for the largest component ($4.12 \pm .24 \mu\text{sec}$) agrees very well with the results of Jeunehomme⁵ for $v' = 3$ at the same pressure. The value for the second component also agrees well with the major unidentified contribution to the First-Positive system. That is, Jeunehomme found an effective lifetime of $17.9 \pm 3.0 \mu\text{sec}$ while the results from the present analysis give $21.0 \pm 3.8 \mu\text{sec}$.

3. The Meinel Bands of N₂⁺

The analysis of the Meinel Band system of N₂⁺ was the primary reason this program was developed. A number of cases containing one and two decay components have been analyzed and a few representative examples are given below.⁶

a. One Component

Figure 9 shows the input data which has been smoothed once and resulting best fit to low-pressure lifetime data of the (2,0) Meinel band. In this case, one component is the only reasonable fit since any attempt to fit two components resulted in two components of the same value as the single component.

b. Two Components

Figure 10 shows the input data (points) which has been smoothed once, best two component fit (solid line) and best single component fit (dashed line). The two component fit

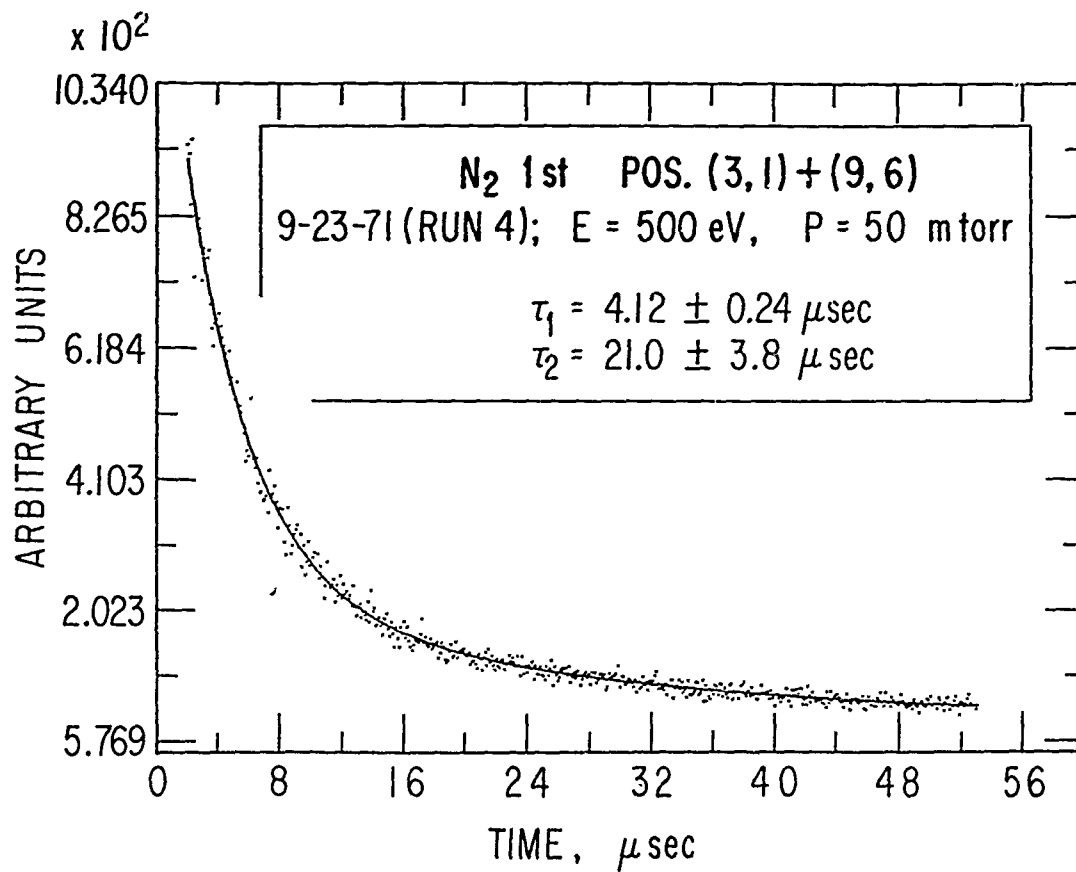


Fig. 8 Fluorescent decay data and the best fit to them for the (3,1) + (9,6) bands of the N_2 1st Positive band system.

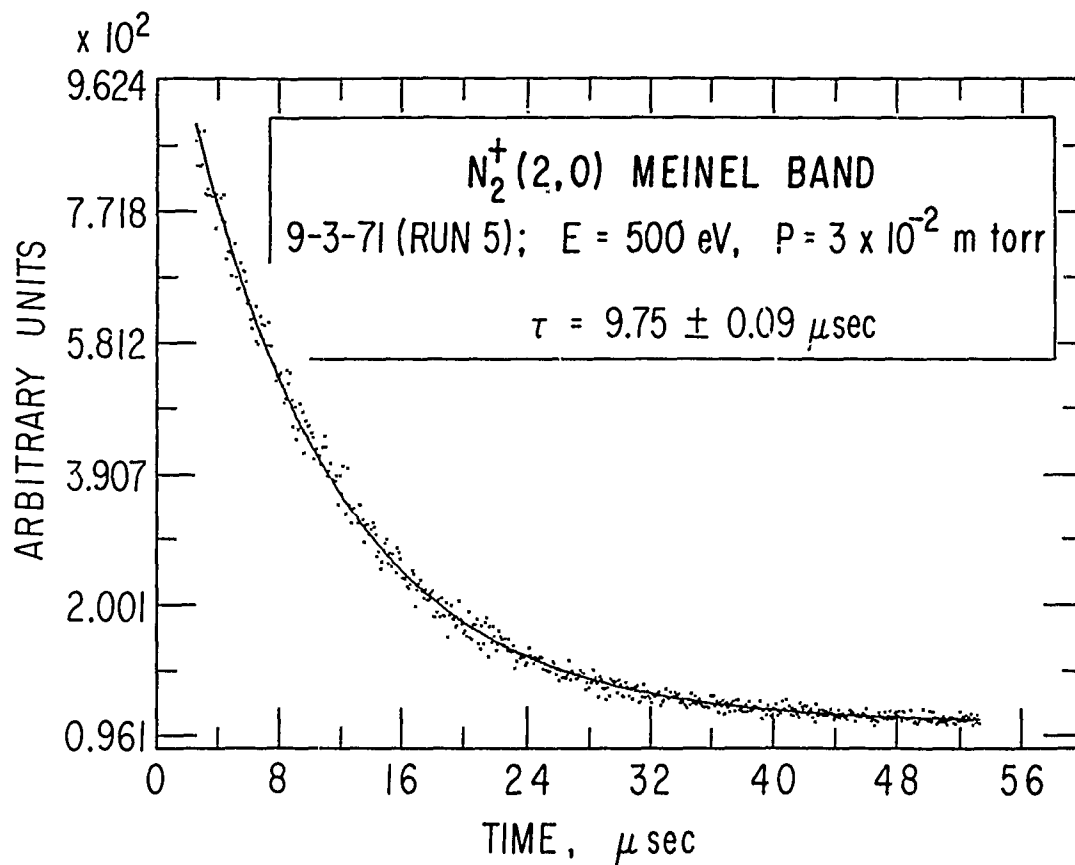


Fig. 9. Low-pressure fluorescent decay data and the best fit to it for the (2, 0) N_2^+ Meinel band.

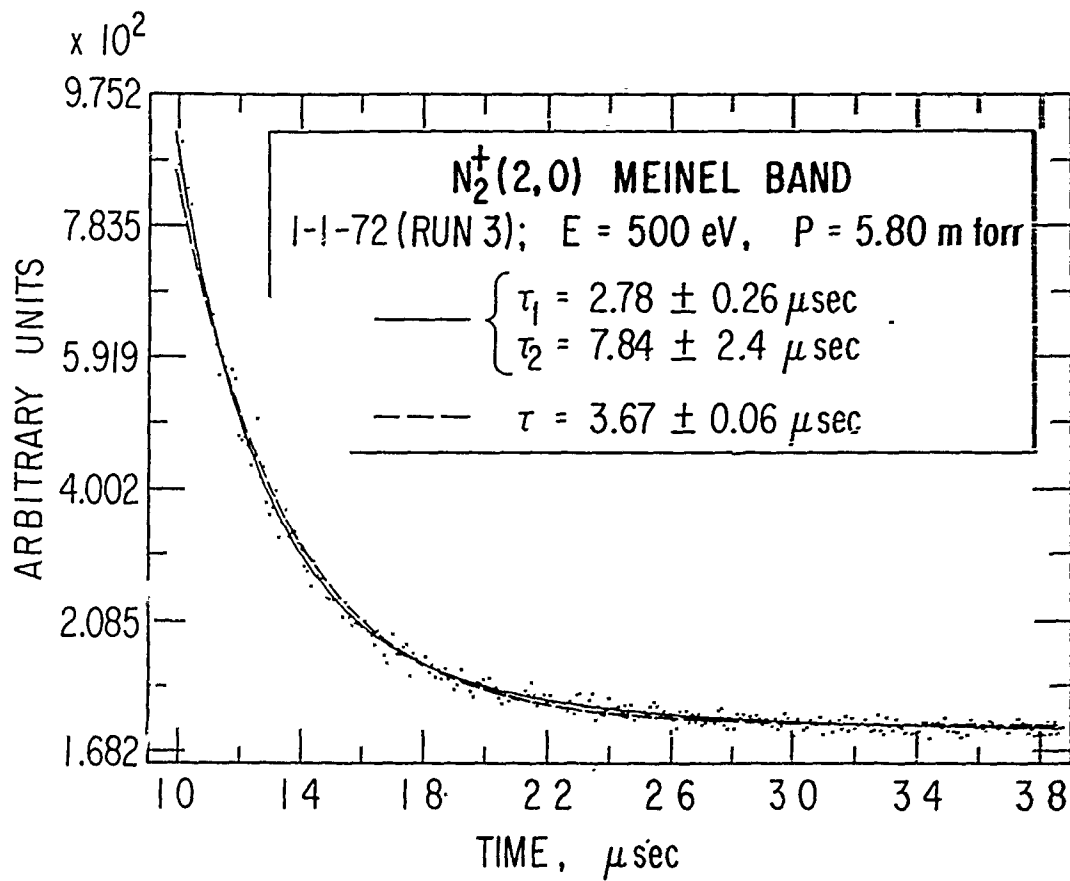


Fig. 10. Same as Fig. 9, but at higher pressure and for which two components are present.

gives a better fit to the data, particularly at early times and in the region 1.2 to 2.6×10^{-5} seconds in the decay curve.

Figure 11 shows results on the same band system as in Figure 10, but taken at a lower pressure and higher beam current. Again two components give a better fit to the data, but in this case the difference is not as apparent from the plots as in Figure 10.

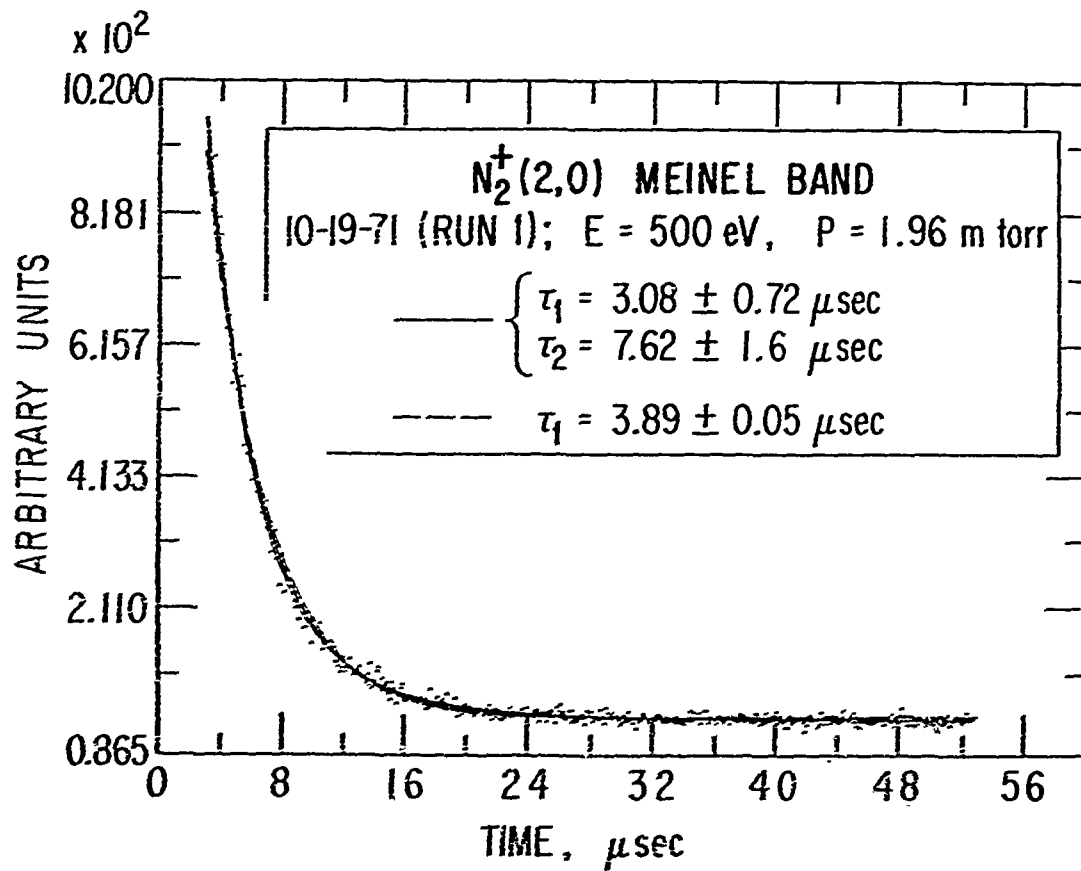


Fig. 11. Same as Fig. 10, but at lower pressure and higher beam current.

APPENDIX

The listing of the program is too long to provide here, but can be obtained by contacting either of the authors at The Space Physics Laboratory, The Aerospace Corporation, P. O. Box 92957, Los Angeles, California 90009; (213) 648-7012/648-5990.

Preceding page blank

REFERENCES FOR SECTION VI

1. W. R. Bennett, Jr., P. J. Kindlmann and G. N. Mercer, *Applied Optics*, Supp. 4 34 (1965).
2. D. A. Meeter, GAUSHAUS, Univ. of Wisconsin; Modified by H. J. Wertz of Aerospace Corp. (1968).
3. CDC 7600 (Namelist) FORTRAN RUN REFERENCE MANUAL
Publication No. 60360700 (1971).
4. The relation $C_j \approx \frac{N(t=0)}{\Delta t} \times (\% \text{ contribution to } \tau_j)$ should be considered when specifying initial guesses and limits.
5. M. Jeunehomme, *J. Chem. Phys.* 45, 1305 (1960); (See his Fig. 2).
6. Data provided by Drs. W. Pendleton and L. Weaver of Utah State University.

Preceding page blank

VII. CONCLUSIONS

Through the combined experimental and theoretical research efforts discussed in the previous sections, a good deal of new information concerning the excitation and radiative processes of the N_2^+ Meinel system has been obtained. A model has been suggested (Section II) for the population of the levels of the $A^2\Pi_u$ state in which autoionization (Section IV) plays an important role. Some insight into goals a) [excitation paths], b) [excitation cross sections,] and c) [emission paths and processes] has thus been gained but more work must be done before quantitative details can be obtained. In Section III, transition probabilities and oscillator strengths were obtained from the newly determined lifetimes for the A-state. These results are basic to the successful completion of goal c) [emission paths and processes] and the interpretation of atmospheric Meinel band emissions. The quenching processes for the A-state are presently being studied experimentally and when results become available, they can be combined with what is currently known [Section V] about the quenching of N_2^+ ($B^2\Sigma_u^+$) and CO^+ ($A^2\Pi$) to satisfy goal e) [collisional quenching cross sections] and the role of quenching of the B-state in goal a) [excitation paths.] The work of Holland and Maier at Los Alamos has resulted in important information about the emission cross sections for the Meinel system [goal d].

At this point, goal f) [radiative lifetimes] and the major portion of goal c) [emission paths and processes] are essentially complete. Experimental measurements on the quenching cross sections and on the emission

Preceding page blank

cross sections need to be performed to complete goals d) and e). Additional theoretical work should be done to determine quantitatively the role of auto-ionization in those processes for goals a), b) and c). Goal g [absolute fluorescence efficiencies] should then follow from the successful completion of these unfinished tasks.